

THE EFFECT OF GAS PRODUCTION RATE
ON THE PERFORMANCE OF PARTIAL
WATER DRIVE-GAS RESERVOIR

by

HASSAN S. AL-HASHIM

CLOSED RESERVE
ARTHUR LAKES LIBRARY
COLORADO SCHOOL OF MINES
GOLDEN, COLORADO 80401

ProQuest Number: 10781120

All rights reserved

INFORMATION TO ALL USERS

The quality of this reproduction is dependent upon the quality of the copy submitted.

In the unlikely event that the author did not send a complete manuscript and there are missing pages, these will be noted. Also, if material had to be removed, a note will indicate the deletion.



ProQuest 10781120


Published by ProQuest LLC (2018). Copyright of the Dissertation is held by the Author.


All rights reserved.

This work is protected against unauthorized copying under Title 17, United States Code
Microform Edition © ProQuest LLC.


ProQuest LLC.
789 East Eisenhower Parkway
P.O. Box 1346
Ann Arbor, MI 48106 – 1346

An Engineering Report submitted to the Faculty and the Board of Trustees of the Colorado School of Mines in partial fulfillment of the requirements for the degree of Master of Engineering.

Signed: 
Hassan S. Al-Hashim

Approved: 
D.M. Bass
Thesis Advisor and
Head of Petroleum Engineering
Department

Golden, Colorado

Date: , 1979

CONTENTS

	Page
CONCLUSION-----	1
INTRODUCTION-----	3
LITERATURE REVIEW-----	4
MATHEMATICAL CONSIDERATION-----	7
SUMMARY AND DISCUSSION OF THE RESULTS-----	12
DATA USED IN THIS STUDY-----	17
CALCULATION PROCEDURE-----	19
ACKNOWLEDGEMENTS-----	52
REFERENCES-----	53

TABLES AND FIGURES

	Page
Table 1	
Sample partial water drive-gas reservoir performance for $P_i = 5,000$ psi, $G = 100$ BSCF, $C_f = 4.0 \times 10^{-6}$ psi ⁻¹ , $Q = 25$ MMSCF/D, and $R_a/R_g = 6.0$ -----	22
Figure 1	
1 Schematic sketch of simplified radial flow model-----	7
2 Water influx performance for $P_i = 5,000$ (psi), $G = 10$ BSCF, $Q = 2.5$ MMSCF/D, $C_f = 4.0 \times 10^{-6}$ psi ⁻¹ and various R_a/R_g -----	23
3 Water influx performance for $P_i = 10,000$ (psi), $G = 10$ BSCF, $Q = 2.5$ MMSCF/D, $C_f = 4.0 \times 10^{-6}$ psi ⁻¹ , and various R_a/R_g -----	24
4 Water influx performance for $P_i = 10,000$ (psi) $R_a/R_g = 2.0$, $G = 100$ BSCF, $Q = 25$ MMSCF/D, $C_f = 4.0 \times 10^{-6}$ psi ⁻¹ -----	25
5 Water influx performance for $P_i = 10,000$ (psi), $R_a/R_g = 3.0$, $G = 100$ BSCF, $Q = 25$ MMSCF/D, $C_f = 4.0 \times 10^{-6}$ psi ⁻¹ -----	26
6 Water influx performance for $P_i = 10,000$ psi $R_a/R_g = 4$, $G = 100.0$ BSCF, $Q = 25$ MMSCF/D, $C_f = 4.0 \times 10^{-6}$ psi ⁻¹ -----	27
7 Water influx performance for $P_i = 10,000$ psi, $R_a/R_g = 6.0$, $G = 100$ BSCF, $Q = 25$ MMSCF/D, $C_f = 4.0 \times 10^{-6}$ psi ⁻¹ -----	28

Figures continued

8	P/Z Performance for $P_i = 5,000$ psi, $P_i = 10,000$ psi, $G = 10.0$ BSCF, $Q = 2.5$ MMSCF/D, $C_f = 8.0 \times 10^{-6}$ psi ⁻¹ -----	29
9	Effect of field production rate on gas recovery for $P_i = 5,000$ psi, $G = 10.0$ BSCF, $C_f = 4.0 \times 10^{-6}$ psi ⁻¹ -----	30
10	Effect of field production rate on P/Z performance for $P_i = 5,000$ psi, $G = 100$ BSCF, $C_f = 4.0 \times 10^{-6}$ psi ⁻¹ , and various R_a/R_g -----	31
11	Effect of field production rate on P/Z performance, for $P_i = 10,000$ psi, $G = 10$ BSCF, $C_f = 4.0 \times 10^{-6}$ psi ⁻¹ and various R_a/R_g -----	32
12	P/Z performance for $P_i = 10,000$ psi, various R_a/R_g , various field production rate, $G = 100$ BSCF, $C_f = 4.0 \times 10^{-6}$ psi ⁻¹ -----	33
13	Effect of formation compressibility on the P/Z performance for $P_i = 5,000$ psi, $P_i = 10,000$ psi, $G = 10$ BSCF, $Q = 2.50$ MMSCF/D and $R_a/R_g = 2.0$ -----	34
14	Gas-water contact performance for $P_i = 5,000$ psi, $G = 10$ BSCF, $Q = 2.5$ MMSCF/D, $C_f = 4.0 \times 10^{-6}$ psi ⁻¹ -----	35
15	Gas-water contact performance for $P_i = 5,000$ psi, $G = 100$ BSCF, $Q = 25$ MMSCF/D, $C_f = 4.0 \times 10^{-6}$ psi ⁻¹ , and various R_a/R_g -----	36

Figures continued

- 16 Gas-water contact performance, for $P_i =$
 10,000 psi, $G = 10$ BSCF, $Q = 2.5$ MMSCF/D,
 $C_f = 4.0 \times 10^{-6}$ psi⁻¹, and various R_a/R_g ----- 37
- 17 Gas-water contact performance for $P_i =$
 10,000 psi, $G = 100$ BSCF, $Q = 25$ MMSCF/D,
 $C_f = 4.0 \times 10^{-6}$ psi⁻¹, and various R_a/R_g ----- 38
- 18 Effect field production rate on the
 gas-water contact performance for $P_i =$
 5,000 psi, $G = 100$ BSCF, $C_f = 4.0 \times 10^{-6}$
 psi⁻¹, and various R_a/R_g ----- 39
- 19 Effect of R_a/R_g on (W_e - Gas-water contact)
 performance for $P_i = 5,000$ psi, $G = 10$ BSCF,
 $Q = 2.5$ MMSCF/D, $C_f = 4.0 \times 10^{-6}$ psi⁻¹----- 40
- 20 Effect of R_a/R_g on (W_e - Gas-water contact)
 performance for $P_i = 5,000$ psi, $G = 100$ BSCF,
 $Q = 25$ MMSCF/D, $C_f = 4.0 \times 10^{-6}$ psi⁻¹----- 41
- 21 Effect of R_a/R_g on (W_e - Gas-water contact)
 performance for $P_i = 10,000$ psi, $G = 100$ BSCF,
 $Q = 25$ MMSCF/D, $C_f = 4.0 \times 10^{-6}$ psi⁻¹----- 42
- 22 Effect of R_a/R_g on (W_e - cum. pore volume
 invaded) performance, for $P_i = 5,000$ psi, $G =$
 10 BSCF, $Q = 2.5$ MMSCF/D, $C_f = 4.0 \times 10^{-6}$ psi⁻¹----- 43

Figures continued

23 Effect of R_a/R_g on (W_e - cum. pore volume invaded) performance, for $P_i = 5,000$ psi, $G = 100$ BSCF, $Q = 25$ MMSCF/D, $C_f = 4.0 \times 10^{-6}$ psi⁻¹,----- 44

24 Effect of R_a/R_g on (W_e - cum. pore volume invaded) performance for $P_i = 10,000$ psi, $G = 10$ BSCF, $Q = 2.5$ MMSCF/D, $C_f = 4.0 \times 10^{-6}$ psi⁻¹----- 45

25 Effect of R_a/R_g on (W_e - cum. pore volume invaded) performance for $P_i = 10,000$ psi, $G = 100$ BSCF, $Q = 25$ MMSCF/D, $C_f = 4.0 \times 10^{-6}$ psi⁻¹----- 46

26 Effect of the expansion of the trapped gas in the water invaded zone on the cumulative volume invaded. For $P_i = 4,000$ psi, $G = 100$ BSCF, $Q = 25$ MMSCF/D, $C_f = 4.0 \times 10^{-6}$ psi⁻¹, and various R_a/R_g ----- 47

27 Effect of constant and decline gas production rates on the Average Reservoir Pressure Performance for $P_i = 10,000$ psi, $G = 100$ BSCF, $C_f = 4.0 \times 10^{-6}$ psi⁻¹, and $R_a/R_g = 4.0$ ----- 48

28 Effect of constant and decline gas production rates on the Cumulative Gas Recovery for $P_i = 10,000$ psi, $G = 100$ BSCF, $C_f = 4.0 \times 10^{-6}$ psi⁻¹, and $R_a/R_g = 4.0$ ----- 49

Figures continued

29	Effect of Constant and Decline Gas Production Rates on the P.Z Performance for $P_i = 10,000$ psi, $G = 100$ BSCF, $C_f = 4.0 \times 10^{-6}$ psi ⁻¹ and $R_a/R_g = 4.0$ -----	50
30	Simplified flow diagram of calculation procedure-----	51

CONCLUSIONS

Based on the results of this study the following was concluded:

1. When the aquifer size compared to the size of the gas reservoir (R_a/R_g) is less than or equal to 2.0 the effect of the aquifer on the performance of the gas reservoir can be neglected.
2. Regardless of the size of the reservoir when $R_a/R_g > 2.0$ the pressure in the unsteady state water influx equation must be corrected to the original gas-water contact. Failure to do so results in an error over 100 percent in the cumulative water influx which in turn could lead to the wrong conclusions regarding the performance of the gas reservoir.
3. Cumulative gas recovery appeared to be sensitive to the aquifer size (when $R_a/R_g > 2.0$), initial reservoir pressure, and gas production rate. As R_a/R_g and the initial reservoir pressure increases, cumulative gas recovery decreases. The sensitivity to gas production rate increases in the large reservoir as R_a/R_g increases. It appeared to be more sensitive when the production rate is allowed to decline.
4. The declining production rate should be avoided as much as possible in order to maximize cumulative gas recovery and decrease the producing life of the reservoirs.

5. The rate at which the gas-water contact advances is controlled by the aquifer size compared to the size of the gas reservoir, and gas production rate when $R_a/R_g > 3.0$.
6. As R_a/R_g increases the expansion of the trapped gas in the water invaded zone decreases, and could be neglected when $R_a/R_g > 4.0$.
7. The performance of the water drive-gas reservoir must be analyzed for all the possible development and production programs in order to determine the optimum production.

INTRODUCTION

Predicting the advance of a gas-water contact in a water drive-gas reservoir plays an important role in the evaluation, forecasting, and analyzing the reservoir performance.

The purpose of this study was to predict the behavior and the rise of the gas-water contact assuming it remains horizontal; and to determine its effect on ultimate gas recovery. Several factors are recognized to control the rise of the gas-water contact. Some of the more important factors are the size of the aquifer, gas production rate, initial reservoir pressure, and formation permeability. These factors account for the abandonment of a number of gas reservoirs at extraordinary high pressure.

Several methods have been developed for predicting the volume of water influx into a reservoir, the Van-Everdingen-Hurst method is used in this study.

The performance calculated in this study was based on the material balance equation for a gas reservoir. The gas reservoir pressure was adjusted to the original gas-water contact for the water influx equation, and the trapped gas in the water invaded zone was accounted for in the water invaded region.

LITERATURE REVIEW

Several methods for predicting the depletion performance of water drive-gas reservoirs have been published in the literature ^{14/}.

Bruns et al ^{5/}, studied the effect of water influx on the P/Z-cumulative gas production curves. From their study they concluded that it is dangerous to extrapolate the P/Z charts on a straight line without considering the possibility of water influx.

Agarwal et al ^{7/}, used a material balance model to study the effect of water influx on natural gas recovery. Based on their calculations they concluded that gas recovery depends on (1) the production rate, (2) the residual gas saturation, (3) the aquifer strength, (4) the permeability, and (5) the volumetric sweep efficiency of the encroaching water zone.

An experimental study of residual gas saturation under water drive was performed by Geffen et al ^{12/} in 1952. The results of their experimental study indicated that residual gas saturation under water drive varies from 15 to 50 percent pore space depending on the type of sand used.

Dumoré, J.M. ^{8/} predicted the future behavior of a bottom water drive gas reservoir. In his study he neglected the total compressibility and assumed that (1) all the gas in the reservoir, and the free gas in the water invaded zone to be at the same average reservoir pressure, (2) the rising of the gas-water contact remains horizontal all the time. On the basis of his study he concluded that (1) use of the time-integrated cumulative water influx is a convenient means of calculating water influx into a reservoir, (2) the straight line relationship between P/Z and G_p

obtained from reservoir pressure data in the early life of the reservoir, does not necessarily indicate a depletion-type production mechanism, but is consistent with a moderate water influx, (3) the calculated P/Z curve (in his example of a gas reservoir) deviated very little from the straight line until more than 50 percent of the initial gas in place has been produced, (4) when the pressure dropped to 90 atm (1323 psi) the calculated G_p was about 85 percent of the initial gas in place, and the gas-water contact had risen to about 70 percent of the closure of the reservoir.

Shagroni, M.A. ^{6/}, studied the effect of formation compressibility, and edge water of gas field performance. From the results of his study he concluded that (1) it is incorrect to extrapolate the early part of the P/Z curves as a straight line to P/Z = 0.0 to estimate the initial gas in place without considering the possibility of water influx and the effect of formation compressibility, (2) the sensitivity of the performance curves (P/Z vs. G_p) to formation compressibility increases as the initial reservoir pressure increases, and decreases as the aquifer size increases.

Pepperdine, L. ^{13/} studied the performance of the Devonian gas fields in northeastern British Columbia. The objective of his study was to: establish means of early recognition of water drive gas fields; find the most efficient methods for predicting gas from water drive gas fields; and estimate the recovery efficiency to be expected under various conditions. From the results of the mathematical model and the analysis of the actual field data he concluded that: (1) to achieve maximum recovery of gas the depletion process should be increased as much as possible by production practices, (2) the important factor in the low efficiency of gas recovery was water influx rather than the coning

phenomenon in the portion of the Clarke Lake field that was modelled.

Givens, J.W. ^{14/} used a simulation model to determine the effects of well density, production rates, water influx, water coning, and rock and fluid properties on the depletion performance of dry gas reservoirs with bottom water drive. On the basis of his results he concluded that: (1) the best performance for reservoirs with bottom water drive will not necessarily be obtained by high producing rates; (2) the presence of bottom water drive in gas reservoirs lowers the ultimate recovery and increases the producing life of the gas reservoirs.

MATHEMATICAL CONSIDERATION

In this study the gas reservoir was taken to have radial water drive and idealized geometry. The reservoir was assigned a dip angle of 15 degrees with a geometric shown in Figure 1.

Basic Assumptions:

1. No phase change in the reservoir;
2. No shale water influx;
3. Residual gas saturation in the water invaded zone (S_{grw}) equal to 20%;
4. No gas produced from the water invaded zone;
5. No water production
6. Gas-water contact remains horizontal at all times.

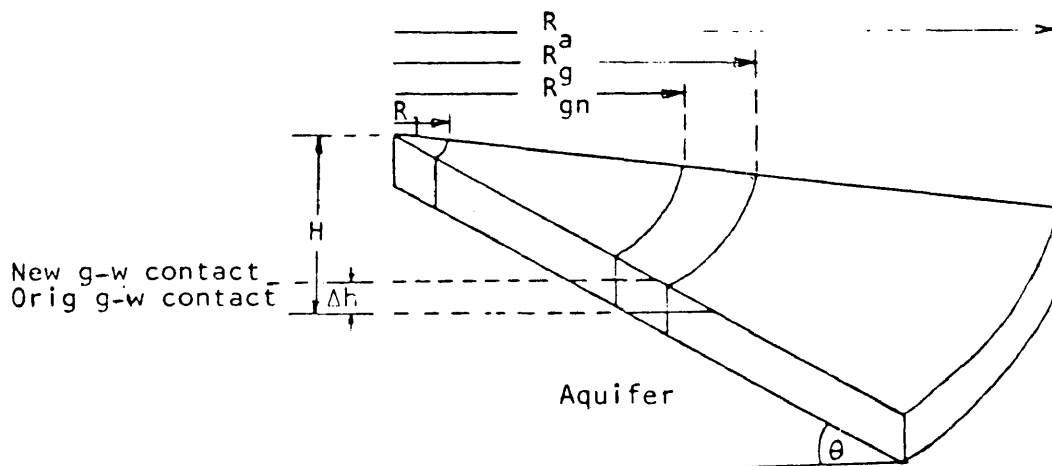


Figure 1. Schematic sketch of simplified radial flow model.

The general form of the material balance equation (MBE) for the gas reservoir under the stated assumptions is

$$G(B_g - B_{gi}) + \frac{GB_{gi}}{1-S_{wi}} (C_w S_{wi} + C_f) (P_i - P) + 5.615 W_e = G_p B_g + 5.615 W_p B_w; \quad (1)$$

where G = standard volume of free gas originally in place

G_p = standard volume of cumulative gas produced

B_{gi} = gas formation volume factor at pressure P_i , cu ft/scf

B_g = gas formation volume factor at pressure P , cu ft/scf

B_w = water formation volume factor, res bbl/surface bbl

C_w = average water compressibility, psi^{-1}

C_f = average formation compressibility, psi^{-1}

P_i = initial reservoir pressure, psi

P = average gas reservoir pressure, psi

S_{wi} = average connate water saturation, fraction

W_e = cumulative water influx, bbls.

W_p = cumulative water production, bbls.

The gas formation volume factor can be written as:

$$B_g = 0.02829 \frac{ZT}{P} \quad (\text{cu ft/scf}) \quad (2)$$

where Z is the gas compressibility factor; and T is the reservoir temperature, $^{\circ}\text{R}$.

Arranging the MBE in terms of P and Z , and assuming no water production equation (3) is obtained

$$W_e = \left[G_p \times Z/P - G \times (Z/P - Z_i/P_i) - G \times \frac{Z_i/P_i}{(1-S_{wi})} \times (C_w S_{wi} + C_f) \right] \times (P_i - P) \left] \frac{1}{A \times 5.615} \quad (3)$$

where $A = T_{ref}/(P_{ref} \times T_{res})$

T_{ref} = reference temperature = 520° R;

P_{ref} = reference pressure = 14.7 psia;

T_{res} = reservoir temperature, °R

when the gas reservoir is considered to be a part of a cone with a fault located at R_1 as shown in Figure 1, the volumetric calculation of the initial gas in place, G , can be obtained by the following equation:

$$GB_{gi} = \Psi\pi\phi h(R_g^2 - R_1^2) (1 - S_{wi}) \quad (5)$$

where Ψ = shape factor = $0.45/0.360$ in this study

ϕ = average reservoir porosity, fraction

h = net pay thickness, ft.

R_g = radius of the internal boundary of the aquifer, ft.

R_1 = radius of the internal boundary of the gas reservoir, ft.

R_1 can be expressed in terms of R_g such that:

$$R_1 = a \times R_g \quad (6)$$

Substituting equation (6) in equation (5) results in:

$$GB_{gi} = \Psi\pi\phi h R_g^2 (1 - a^2) (1 - S_{wi}) \quad (5A)$$

Equation (5A) can be solved for R_g , and the initial pore volume (V_i) if G , P_i , Ψ , ϕ , h , a , and S_{wi} are known.

Knowing R_g , the water influx (W_e) for a radial system can be calculated using the unsteady state water influx equation of Van-Everdingen and Hurst:

$$W_{e_n} = \frac{\psi 2\pi \phi h C_e R_g^2 q}{5.615} \sum_{J=1}^n \left[Q(t_{D_n} - t_{D_{J-1}}) \Delta P_J \right] ; \quad (6)$$

$$\text{where } t_D = \frac{0.006328 k_w t}{\mu_w \phi C_e R_g^2} ; \quad (7)$$

$$\Delta P_J = \frac{(P_{J-2} - P_J)}{2} \quad \text{for } J \geq 2; \text{ and} \quad (8A)$$

$$\Delta P_1 = \frac{P_i - P_J}{2} \quad \text{for } J = 1 \quad (8B)$$

$Q(t_D)$ is the dimensionless water influx function as defined by Van-Everdingen and Hurst^{10/}.

The cumulative pore volume of the water invaded zone can be calculated by the following equation:

$$\begin{array}{l} \text{Pore Volume of Water} \\ \text{Invaded Zone, Bbl} \end{array} \quad V_{w_n} = \sum_{J=1}^n \Delta V_{w_J} \quad (9)$$

$$\text{where } \Delta V_{w_J} = \left\{ (W_{e_J} - W_{e_{J-1}}) - (W_{pB_w})_J + (W_{pB_w})_{J-1} \right.$$

$$\left. + \left[\sum_{i=1}^{J-1} \frac{\Delta V_{wi}}{B_{gi}} S_{grw} \right] \frac{(B_{gJ} - B_{g_{J-1}})}{5.615} \right\}$$

$$\div (1 - S_{wi} - S_{grw}) \quad (10)$$

Having determined the cumulative pore volume of the water invaded zone, the current pore volume containing free gas (V_c) above the gas-water contact can be obtained by the following equation:

$$V_{c_n} = V_i - \sum_{J=1}^n \Delta V_{w_J} \quad (11)$$

And the corresponding rise of the gas-water contact (Δh_n) can be obtained from the following relation:

$$\Delta h_n = (R_g - R_{g_n}) \sin \theta \quad (12)*$$

Where R_{g_n} is the current reservoir radius at the new gas-water contact. Using the foregoing equations, the pressure at the original gas-water contact can be calculated with equation (13).

$$P_{n@orig \text{ g-w contact}} = P_n + 0.433 \Delta h_n \times \gamma_w + \frac{dW_e}{dt} \cdot \frac{\mu_w \ln(R_g/R_{g_n})}{0.00708 k_{rw} h \psi} \quad (13)$$

where γ_w is the specific gravity of the water, and μ_w is the viscosity of the water in cp, and k_{rw} is the relative permeability to water in the water invaded-zone.

*This equation is valid until $R_{g_n} = R_1 + h/2 \sin \theta \cos \theta$

SUMMARY AND DISCUSSION OF THE RESULTS

The results of the calculations for small ($G=10$ BSCF) and relatively large ($G=100$ BSCF) gas reservoirs are shown in Figures 1 through 29 and summarized below.

Figures 2 through 7 show the performance of the cumulative water influx (W_e) calculated using average gas reservoir pressure corrected to the original gas-water contact. The effect of the initial reservoir pressure and aquifer size are also shown in these figures. From these figures the following results were obtained:

1. Regardless of the gas reservoir size when $R_a/R_g < 3.0$ the performance of the gas reservoir is not affected by the aquifer, and the average reservoir pressure can be used to calculate the cumulative water influx. The aquifer can also be treated as a finite storage tank. This result justifies the first assumption of Dumoré, J.M.^{8/} in his calculation of the cumulative water influx. However, when R_a/R_g increased from 3.0 to 6.0 the difference between the average reservoir pressure and the pressure calculated at the original gas-water contact increased from a negligible amount to more than 4000 psi in some cases. This indicates that Dumoré's first assumption can not be used when $R_a/R_g > 2.0$.
2. When $R_a/R_g = 6.0$ the effect of the aquifer boundary was noted only for small gas reservoirs. This is because the area of

disturbance which created by the flowing of water across the gas-water contact reached the outer boundary in the small aquifer faster than that in the the large aquifer.

Figures 8 through 12 show the response of the P/Z curves to the initial reservoir pressure and aquifer size. This response shows that as R_a/R_g and the initial reservoir pressure increase the average reservoir pressure is maintained at higher levels. In regard to pressure level, the calculated gas recovery at a field production rate of 25 MMSCF/D ranges from 76 percent for an initial reservoir pressure of 10,000 psi to in excess of 92 percent for an initial reservoir pressure of 5,000 psi (Figures 10 and 12). Cumulative gas recovery was found to be sensitive to gas production rate only when $R_a/R_g > 2.0$. This result indicates that recovery in depletion-type gas reservoirs is not sensitive to gas production rate even with some edge water influx.

In general as R_a/R_g and initial reservoir pressure increase the cumulative gas recovery decreases and becomes more sensitive to gas production rate and aquifer permeability.

Although the effect of aquifer permeability on the gas reservoir performance is not of interest in this study, it is worthwhile to mention some results obtained from this study regarding the subject.

The effect of aquifer permeability on gas reservoir performance with water influx was studied by Bruns et al.^{5/} for finite aquifers. They showed that for $R_a/R_g = 1.5$ the effect of the aquifer on the performance of the gas reservoir is negligible for the given water compressibility of $3.0 \times 10^{-6} \text{ psi}^{-1}$, porosity of 0.25 and water viscosity of 1.0 regardless

of the permeability.

This result agrees with the results obtained from this study for $R_a/R_g = 2.0$.

Agarwal et al^{7/} showed that the aquifer permeability has a great effect on the gas reservoir performance and on the cumulative gas recovery for an infinite aquifer. They also showed the effect of gas production rate on the cumulative gas recovery for various aquifer permeabilities and concluded that cumulative gas recovery decreases as the permeability increases.

In this study an aquifer permeability of 300 md was used and as R_a/R_g increased from 2 to 6, the cumulative gas recovery appeared to be sensitive to gas production rate. Figure 18 shows this effect for production rates of 1 MMSCF/D per 4, 6, and 8 BSCF of initial gas in place respectively.

Figures 14 through 21 show the effect of the aquifer size initial reservoir pressure, and gas production rate on the rate at which the gas-water contact advanced.

In response to the pressure drop in the gas reservoir, because of gas production, the aquifer reacts to offset or retard the pressure decline by providing a source of water influx or encroachment by the expansion of the water and aquifer rock compressibility. Consequently, the gas-water contact advances entrapping some gas behind it. As the reservoir pressure continues to decline the gas-water contact continues to advance and the trapped gas expands resulting in an acceleration of the rate at which the gas-water contact advances. From the above figures (14-21) it can be seen that the rate at which the gas-water contact advances was controlled by the rate of water influx and the expansion of the trapped gas in the water invaded zone. As R_a/R_g increases the

expansion of the trapped gas decreases, and can be neglected when $R_a/R_g > 4.0$.

Figures 27 through 29 present the results when the initial rate of production was the same but one rate was maintained constant and the other rate declined in proportion to the volume of the reservoir not invaded by water. The constant rate performance was analyzed and discussed in detail elsewhere in this study, and presented here for comparison purposes only.

Comparing the performance of the gas reservoir predicted with the declining and the constant production rates showed agreements in the first two years. However, after about two years of production history the following results were noted: (1) the average gas reservoir pressure declined faster for the constant production rate; and (2) the cumulative gas recovery decreased from 82 to 73 percent of the initial gas in place when the initial production rate was allowed to decline with time. In the same time the producing life of the gas reservoir increased from 9 years to about 27 years.

The above noted results for the declining production rate agree with that presented by Givens, J.W.^{14/} in his study with bottom water drive.

From the above results it is recognized that the behavior of the average reservoir pressure for the declining production rate is more like what most people associate with a water drive gas reservoir. However, the behavior of the average reservoir pressure for the constant production rate could lead to the conclusions that indicate the absence of a water drive. The $P/Z - G_p$ performance shown in Figure 29 for the declining

production rate indicates that special attention should be given when evaluating and analyzing the performance of the gas reservoir. Such attention should not be confused with the effect of formation compressibility, active water drive, and high aquifer permeability.

DATA USED IN THIS STUDY

1. Rock and fluid properties:

- a. Aquifer permeability = 300 md
- b. Porosity = 0.25
- c. Water viscosity = 0.7 cp
- d. Gas specific gravity = 0.65
- e. Formation compressibility = $4 \times 10^{-6} \text{ psi}^{-1}$
= $8 \times 10^{-6} \text{ psi}^{-1}$
= $12 \times 10^{-6} \text{ psi}^{-1}$
- f. Connate water compressibility = $3.5 \times 10^{-6} \text{ psi}^{-1}$
- g. Connate water saturation = 0.25
- h. Residual gas saturation in the water-
invaded zone = 0.2
- i. Gas compressibility factor (Z) is
calculated as a function of Pr and Tr
using ZFACT Subroutine.
- j. Gas formation volume factor (Bg) is
calculated as a function of compressibility
factor (Z), pressure, and temperature using
equation 2, cu ft/SCF.

2. Reservoir and Aquifer conditions:

- a. Reservoir thickness = 30 ft
- b. Shape factor = 1/8
- c. Initial reservoir pressure = 10,000 psi
= 5,000 psi

- d. Relative size of the aquifer R_a/R_g = 2.0
 = 3.0
 = 4.0
 = 6.0
- e. Initial gas in place = 10 BSCF
 = 100 BSCF
- f. Production rate = 1 MMSCF/D per 4,
 6, and 8 BSCF of
 Initial gas in place
- g. Reservoir temperature is calculated as a
 function of initial reservoir pressure using the
 following equation:
 $P_i = 0.6 \times D$;
 $T = 74.0 + 1.7 \times D/100$;
 $T = 74.0 + (1.7 \times P_i)/(0.6 \times 100) + 460.0$ °R.
- h. Reference temperature = 520° R
- i. Reference pressure = 14.7 psia
- j. k_{rw} = 150 md

CALCULATION PROCEDURE

The following steps summarize the calculation procedure:

- A. For a fixed time increase of two months (60.83 days), and a production rate of $0.000125 \times G$ SCF/D, the value of G_p is obtained.
- B. For a specific value of initial reservoir pressure, formation compressibility, R_1/R_g , R_a/R_g , and assumed average reservoir pressure P , the material balance equation, equation (3) is solved

$$W_{e_n} = \left[G_p \times Z/P - G \times (Z/P - Z_i/P_i) - G \times \frac{Z_i/P_i}{(1 - S_{wi})} \right. \\ \left. \times (C_w S_{wi} + C_f)(P_i - P) \right] \frac{1}{A \times 5.615} \quad (3)$$

- C. The cumulative pore volume of the water invaded zone is calculated using equation (9)

$$V_{w_n} = \sum_{J=1}^n \Delta V_{w_J} \quad (9)$$

- D. The remaining pore volume of the gas reservoir is calculated using equation (11)

$$V_{c_n} = V_i - \sum_{J=1}^n \Delta V_{w_J} \quad (11)$$

- E. The gas reservoir radius of the remaining pore volume (R_{g_n}) is calculated using the following equation:

$$R_{g_n} = \sqrt{V_{c_n} / (\Psi \Phi \pi h (1-a^2) (1-S_{wi}))}$$

- F. The rise of the gas-water contact (Δh_n) is calculated using equation (12)

$$\Delta h_n = (R_g - R_{g_n}) \sin \theta \quad (12)$$

- G. The pressure at the original gas-water contact was calculated using equation (13)

$$P \text{ @ orig. g-w contact} = P_n + 0.433 \Delta h_n \times \gamma_w +$$

$$\frac{dW_e}{dt} \times \frac{\mu_w \ln(R_g/R_{g_n})}{0.00708 k_{rw} h \Psi}$$

- H. The Van-Everdingen and Hurst unsteady state water influx equation, equation (6) is solved using the pressure at the original gas-water contact.

$$W_{e_n} = \frac{\Psi 2\pi \Phi C_e h R_g^2}{5.615} \sum_{J=1}^n \left[Q(t_{D_n} - t_{D_{J-1}}) \Delta P_J \right] \quad (6)$$

- I. Steps B through H are repeated assuming another reservoir pressure until the water influx calculated by the MBE, Equation (3), and the unsteady state water influx equation, Equation (6) are in satisfied agreement.

- J. Steps A through I are repeated until the gas reservoir is abandoned.
- K. Steps A through J are repeated for different values of R_a/R_g .
- L. Steps A through K are repeated for different C_f .
- M. Steps A through L are repeated for different gas production rates.
- N. Steps A through M are repeated for different initial reservoir pressure.

TABLE 1

Cumulative Gas Production and Corresponding Properties at Increasing Time Steps of Two Months (60.83 days) for $P_i=5,000$ psi, $G=100$ BSCF, $C_f=4.0 \times 10^{-6}$ psi $^{-1}$, $Q=25$ MMSCF/D, $k_w=300$ md, $S_{grw}=20\%$, and $R_a/R_g=6.0$.

TIME (DAYS)	GF (BSCF)	AUG. RES. PRESSURE (PSI)	POORIG. G W CONT (PSI)	F/Z (PSI)	CUM WE (MMBBL)	CUM PORE VOL. INVADED (MMBBL)	HEIGHT OF G W CONT (FT)
0.000	0.00	5000.00	5000.00	4766.99	0.0000	0.0000	0.00
60.830	1.52	4898.95	4900.60	4899.70	0.0703	0.1273	3.19
121.660	3.04	4809.27	4816.13	4830.71	0.2377	0.4323	10.80
182.490	4.56	4725.26	4737.53	4780.50	0.4525	0.8232	20.58
243.320	6.08	4645.65	4669.36	4724.30	0.7041	1.2813	32.10
304.150	7.60	4569.46	4604.36	4669.57	0.9854	1.7937	45.02
364.980	9.12	4496.08	4543.83	4615.98	1.2921	2.3527	59.17
425.810	10.65	4425.05	4487.13	4563.27	1.6205	2.9517	74.40
486.640	12.17	4356.02	4433.86	4511.24	1.9683	3.5863	90.61
547.470	13.69	4287.51	4380.01	4458.01	2.3192	4.2271	107.07
608.300	15.21	4218.23	4322.79	4404.97	2.6578	4.8462	123.04
669.130	16.73	4148.36	4264.52	4349.83	2.9860	5.4471	138.62
729.960	18.25	4078.25	4206.08	4293.63	3.3073	6.0360	153.96
790.790	19.77	4008.08	4147.75	4236.52	3.6240	6.6174	169.17
851.620	21.29	3938.02	4089.81	4178.61	3.9381	7.1948	184.35
912.450	22.81	3868.19	4032.44	4120.01	4.2512	7.7712	199.58
973.280	24.33	3798.71	3975.72	4060.75	4.5641	8.3482	214.87
1034.110	25.85	3729.48	3919.52	4000.86	4.8774	8.9267	230.32
1094.940	27.37	3660.50	3863.50	3940.29	5.1905	9.5057	245.84
1155.770	28.89	3591.71	3807.59	3879.00	5.5038	10.0844	261.42
1216.600	30.42	3523.05	3751.55	3816.93	5.8136	10.6613	277.04
1277.430	31.94	3454.53	3695.80	3754.10	6.1232	11.2373	292.71
1338.260	33.46	3386.13	3640.08	3690.48	6.4314	11.8120	308.42
1399.090	34.98	3317.83	3584.57	3626.09	6.7383	12.3857	324.18
1459.920	36.50	3249.63	3529.22	3560.90	7.0441	12.9588	340.01
1520.750	38.02	3181.52	3474.16	3494.94	7.3490	13.5318	355.92
1581.580	39.54	3113.49	3419.20	3428.18	7.6529	14.1048	371.91
1642.410	41.06	3045.53	3364.51	3360.63	7.9562	14.6784	388.00
1703.240	42.58	2977.60	3309.80	3292.27	8.2585	15.2522	404.18
1764.070	44.10	2909.69	3255.31	3223.10	8.5600	15.8268	420.47
1824.900	45.62	2841.75	3200.78	3153.10	8.8607	16.4020	436.87
1885.730	47.14	2773.80	3146.57	3082.27	9.1607	16.9787	453.40
1946.560	48.66	2705.77	3092.16	3010.59	9.4599	17.5564	470.06
2007.390	50.18	2637.66	3038.12	2938.07	9.7585	18.1363	486.87
2068.220	51.71	2569.43	2983.97	2864.69	10.0566	18.7193	503.84
2129.050	53.23	2501.04	2929.90	2790.44	10.3540	19.3030	520.99
2189.880	54.75	2432.48	2876.05	2715.32	10.6512	19.8891	538.35
2250.710	56.27	2363.69	2821.91	2639.30	10.9478	20.4800	555.91
2311.540	57.79	2294.64	2768.12	2562.40	11.2442	21.0787	573.72
2372.370	59.31	2225.29	2714.09	2484.58	11.5403	21.6796	591.78
2433.200	60.83	2155.59	2660.22	2405.84	11.8362	22.2864	610.14
2494.030	62.35	2085.49	2606.26	2326.17	12.1320	22.8999	628.82
2554.860	63.87	2014.95	2552.25	2245.55	12.4277	23.5210	647.87
2615.690	65.39	1943.91	2498.27	2163.97	12.7234	24.1510	667.32
2676.520	66.91	1872.30	2444.18	2081.42	13.0192	24.7911	687.23
2737.350	68.43	1800.07	2390.07	1997.87	13.3150	25.4430	707.65
2798.180	69.95	1727.15	2335.89	1913.31	13.6110	26.1085	728.66
2859.010	71.48	1653.48	2281.81	1827.73	13.9073	26.7901	750.35
2919.840	73.00	1578.96	2227.47	1741.09	14.2036	27.4901	772.81
2980.670	74.52	1503.53	2173.29	1653.39	14.5002	28.2121	796.18
3041.500	76.04	1427.10	2119.06	1564.59	14.7969	28.9602	820.62
3102.330	77.56	1349.56	2064.80	1474.67	15.0936	29.7394	846.32
3163.160	79.08	1270.84	2011.07	1383.61	15.3904	30.5569	873.56
3223.990	80.60	1190.81	1957.06	1291.37	15.6867	31.4208	902.67
3284.820	82.12	1109.37	1903.93	1197.92	15.9824	32.3434	934.13
3345.650	83.64	1026.39	1851.20	1103.23	16.2768	33.3404	968.59
3406.480	85.16	941.75	1799.52	1007.27	16.5693	34.4347	1006.97
3467.310	86.68	855.31	1749.41	909.98	16.8586	35.6598	1050.69
3528.140	88.20	766.91	1701.63	811.35	17.1431	37.0667	1101.90
3588.970	89.72	676.42	1657.32	711.32	17.4202	38.7373	1164.24
3649.800	91.25	583.65	1618.60	609.85	17.6855	40.8125	1244.15
3710.630	92.77	488.40	1589.63	506.92	17.9323	43.5556	1354.55
3771.460	94.29	390.58	1577.25	402.51	18.1476	47.5199	1525.45
3832.290	95.81	290.00	1599.55	296.62	18.3057	54.0908	1849.28

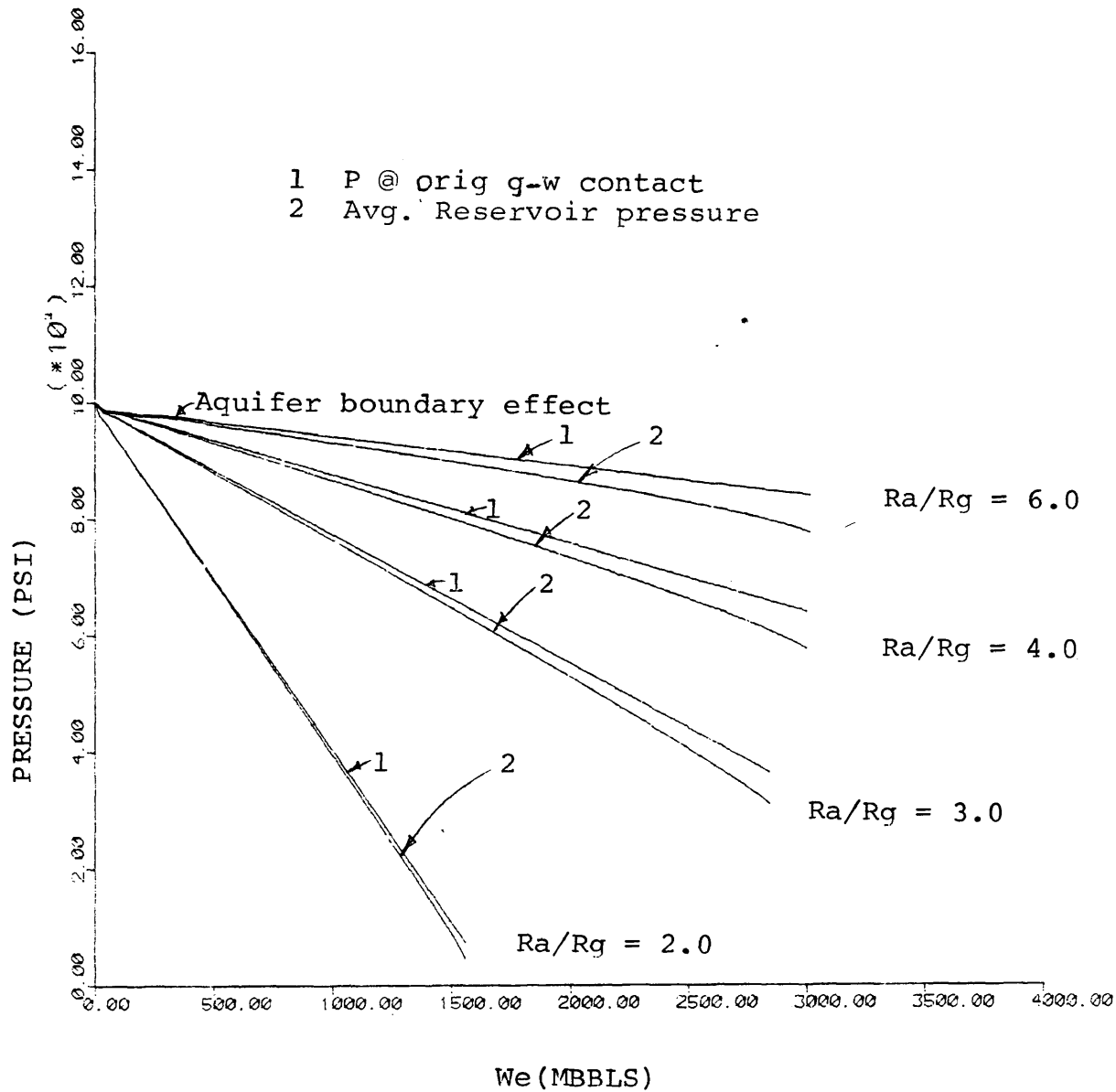


Figure 3. Water Influx Performance for $P_i = 10,000$ psi, $G = 10.0$ BSCF, $Q = 2.5$ MMSCF/D, $C_f = 4.0 \times 10^{-6}$ psi⁻¹, and various Ra/Rg.

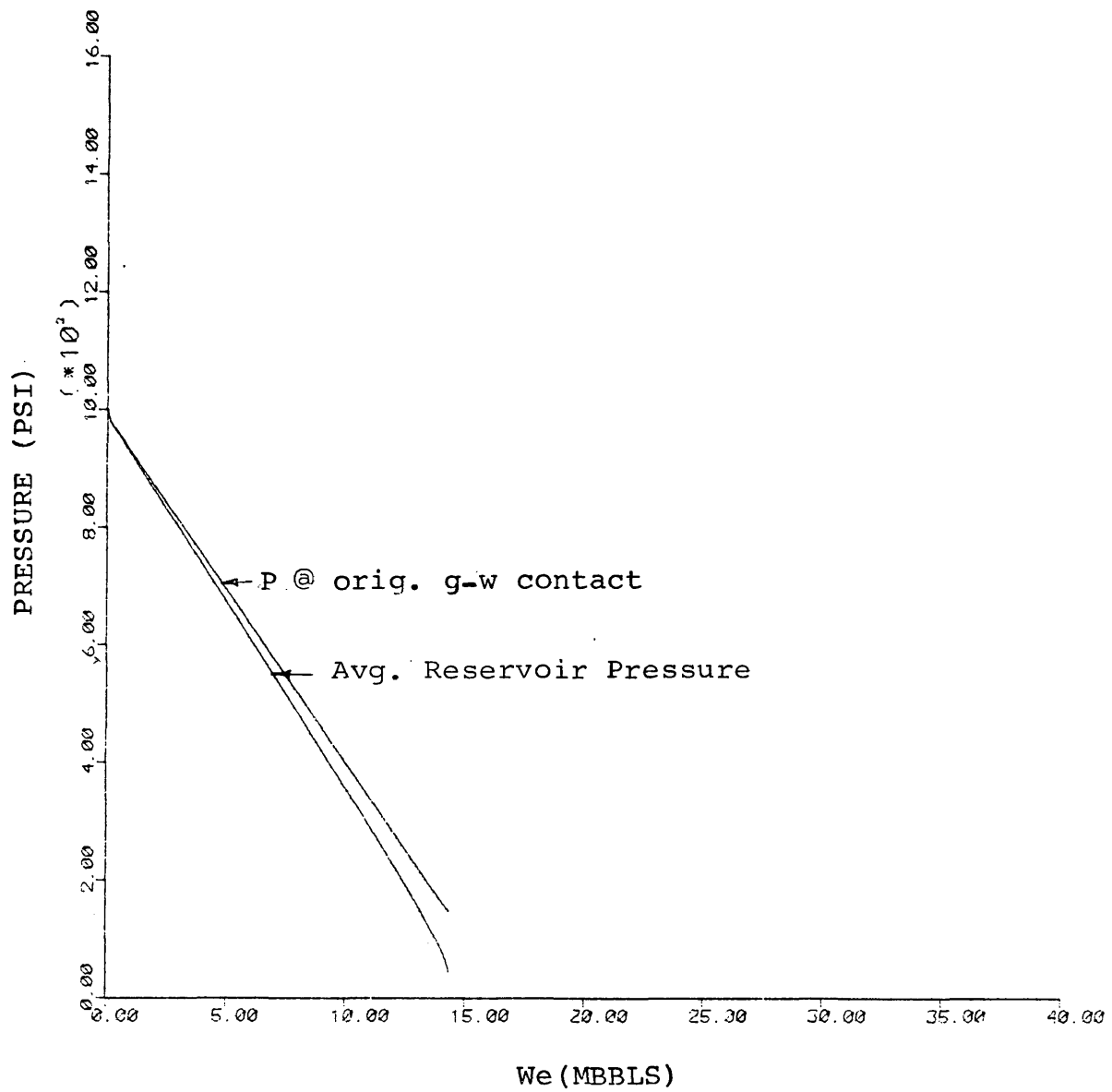


Figure 4. Water Influx Performance for $P_i = 10,000$ psi, $R_a/R_g = 2.0$, $G = 100.0$ BSCF, $Q = 25$ MM SCF/D, and $C_f = 4.0 \times 10^{-6}$ psi⁻¹.

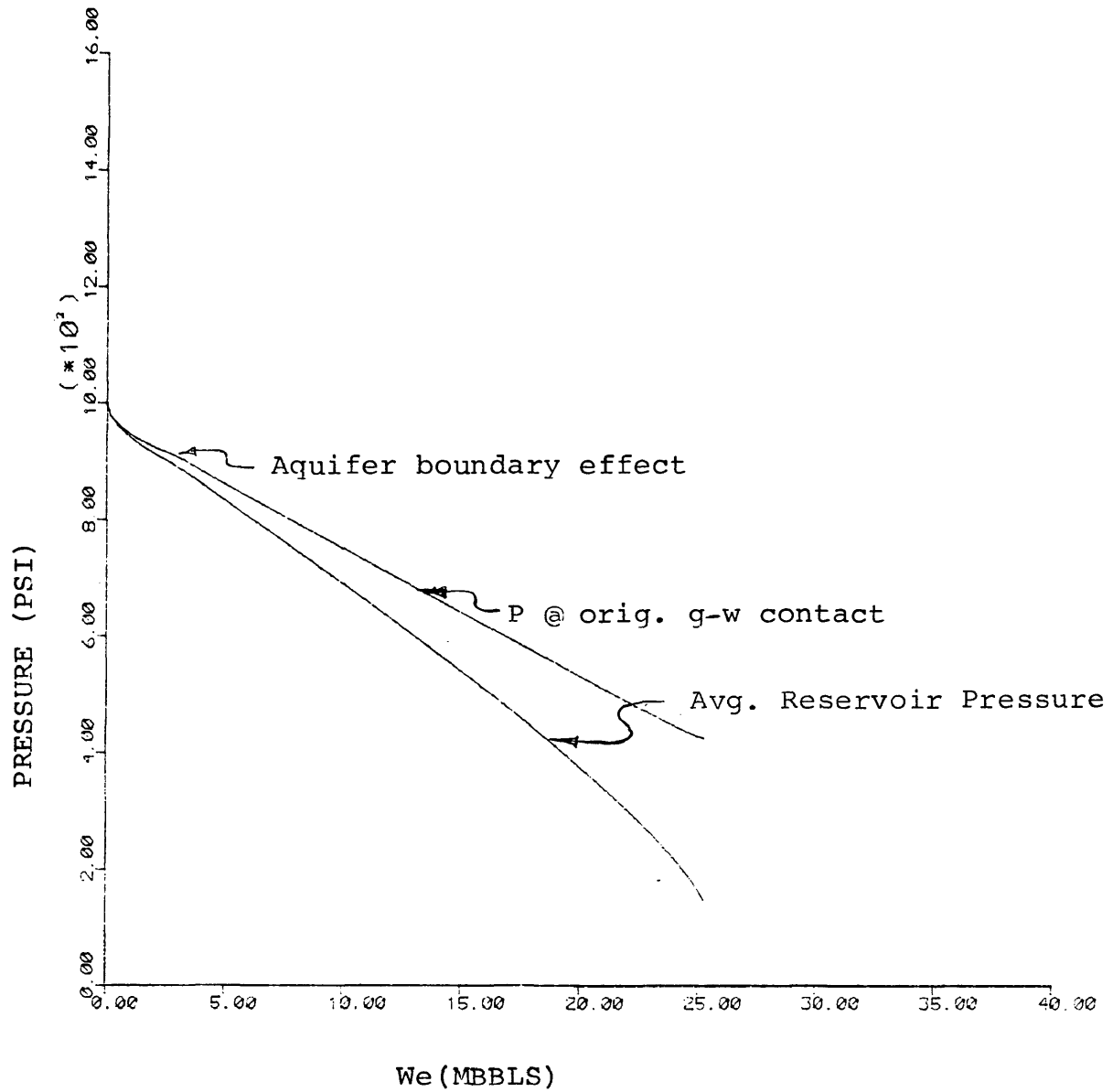


Figure 5. Water Influx Performance for $P_i = 10,000$ psi, $R_a/R_g = 3$, $G = 100.0$ BSCF, $Q = 25$ MMSCF/D, and $C_f = 4.0 \times 10^{-6}$ psi $^{-1}$.

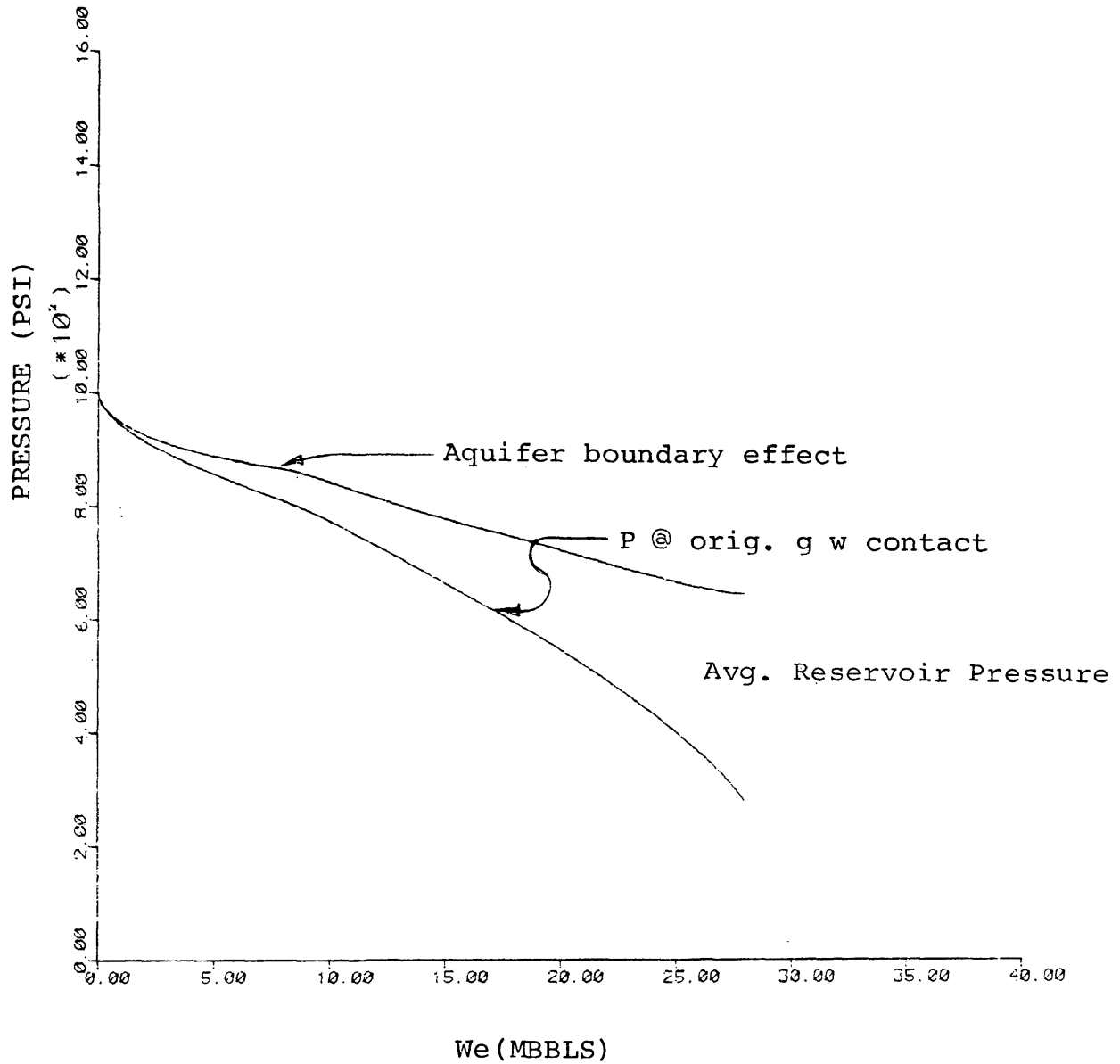


Figure 6. Water Influx Performance for $P_i = 10,000$ psi
 $R_a/R_g = 4$, $G = 100.0$ BSCF, $Q = 25$ MMSCF/D, and
 $C_f = 4.0 \times 10^{-6}$ psi $^{-1}$.

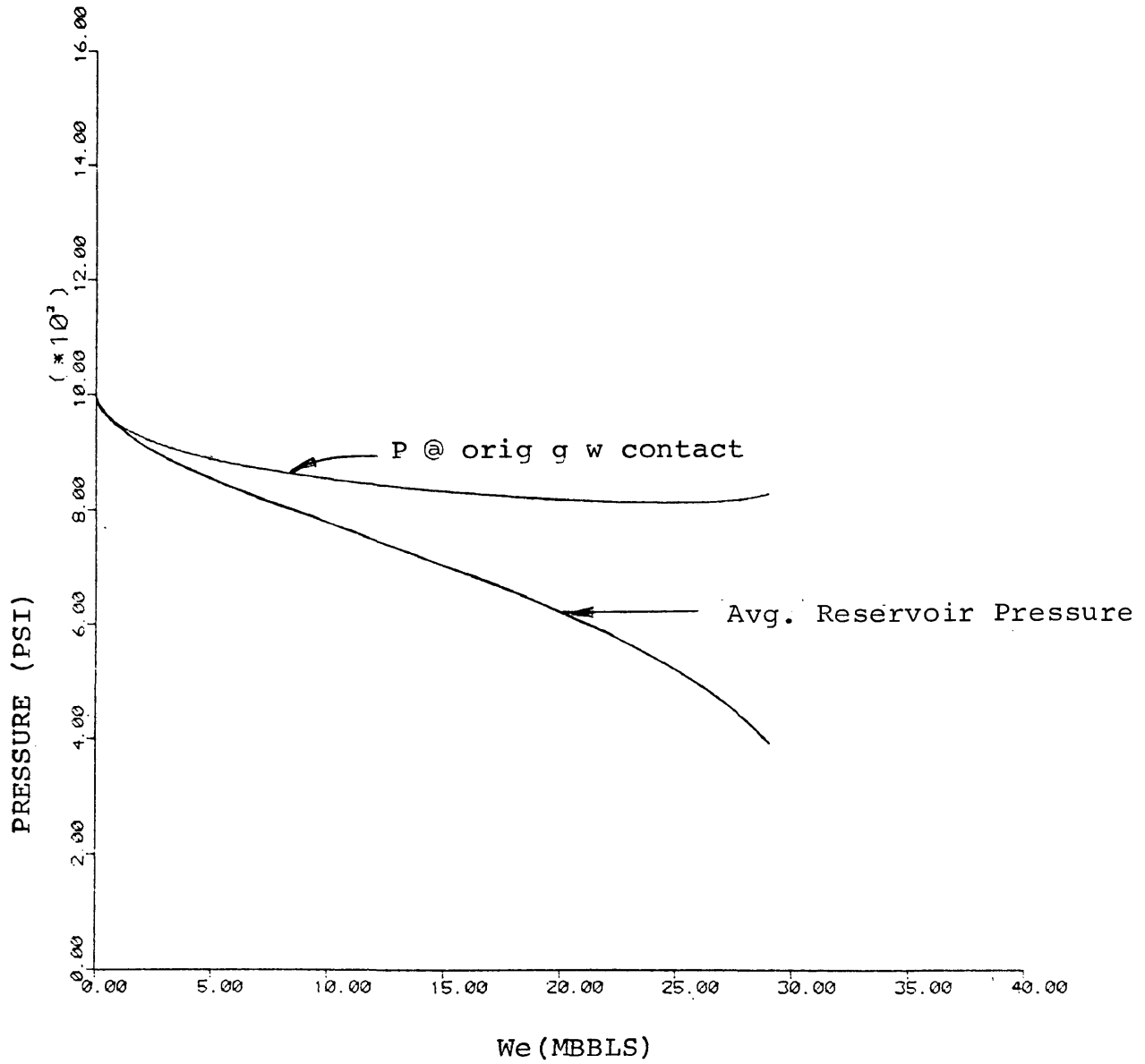


Figure 7 . Water Influx Performance for $P_i = 10,000$ psi, $R_a/R_g = 6.0$, $G = 100.0$ BSCF, $Q = 25$ MMSCF/D, and $C_f = 4.0 \times 10^{-6}$ psi⁻¹.

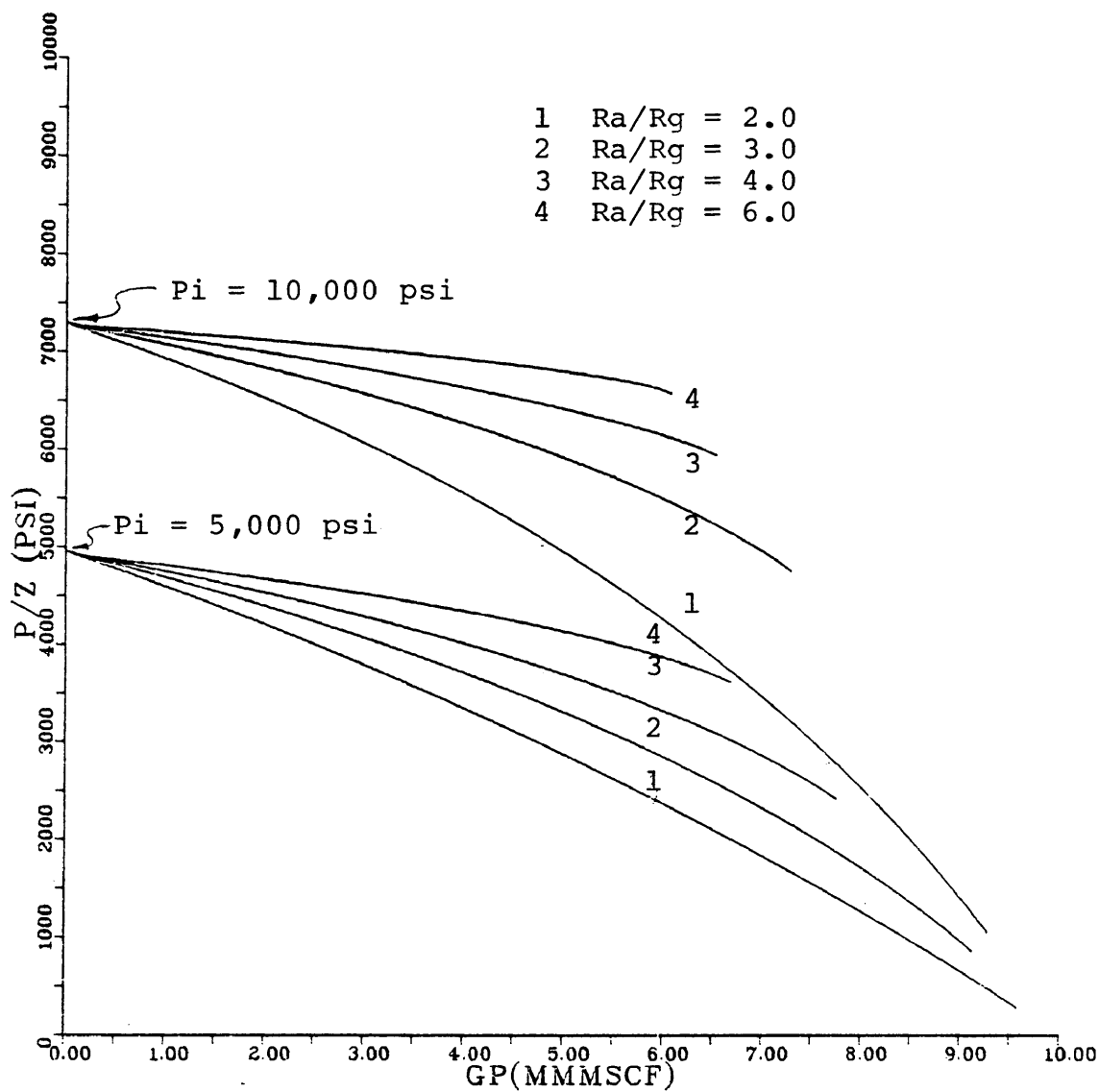


Figure 8. P/Z Performance for $P_i = 5000$ psi, $P_i = 10000$ psi, $G = 10.0$ BSCF, $Q = 2.5$ MMSCF/D, and $C_f = 8.0 \times 10^{-6}$ psi⁻¹.

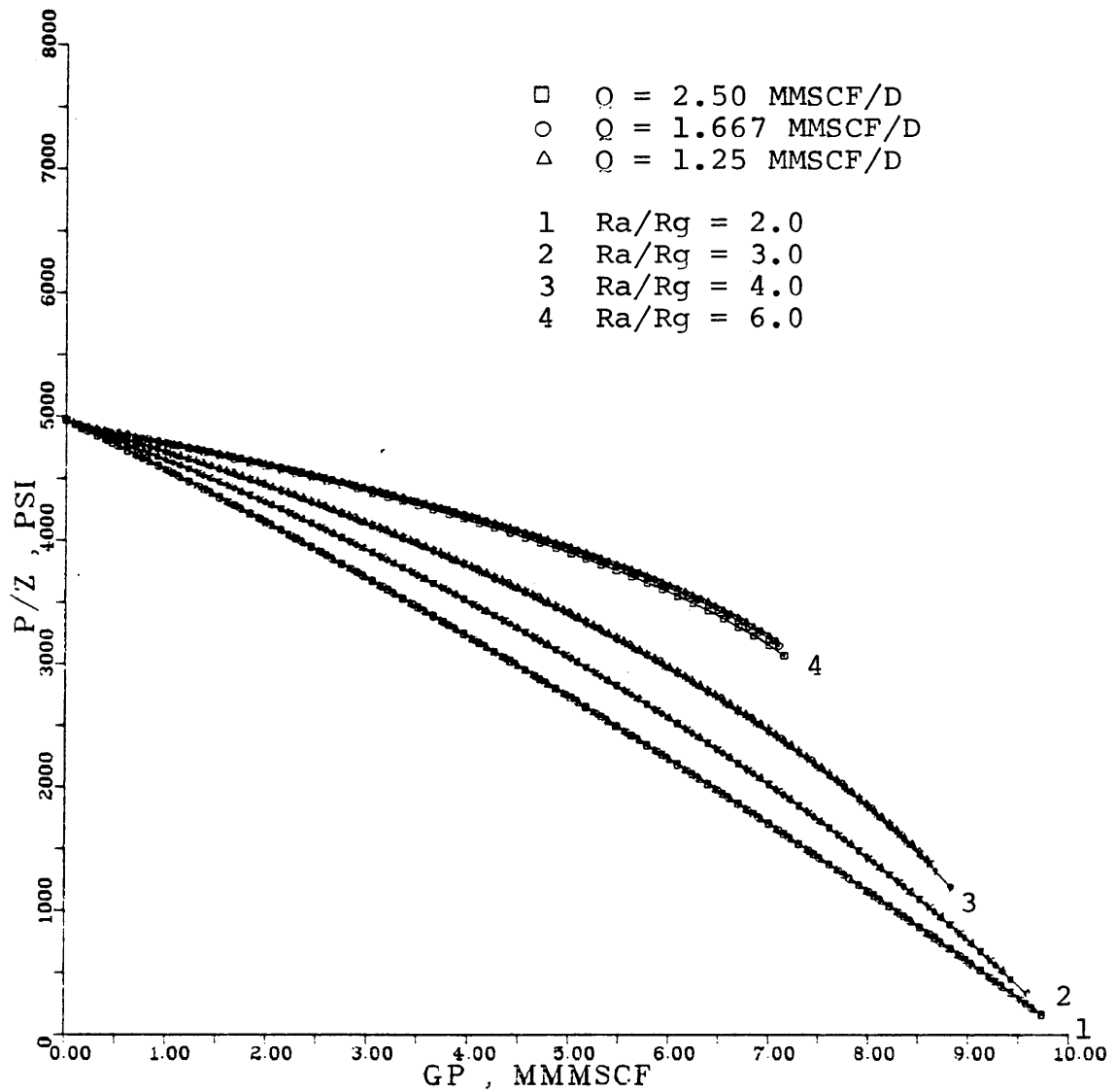


Figure 9. Effect of Field Production Rate on Gas Recovery
 For $P_i = 5,000$ psi, $G = 10.0$ BSCF, and $C_f = 4.0 \times 10^{-6}$ psi⁻¹.

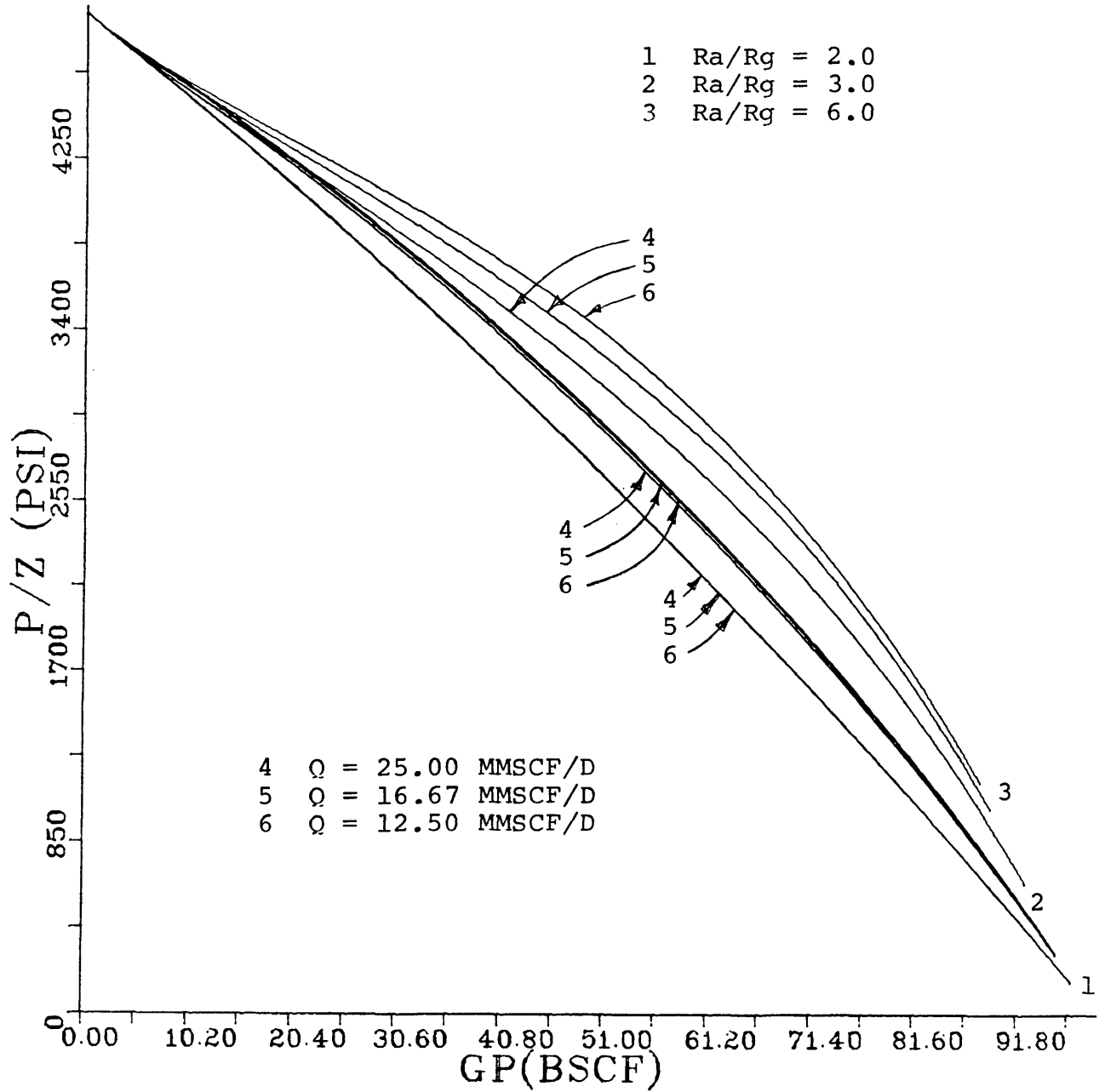


Figure 10. Effect of Field Production Rate on P/Z Performance for $P_i = 5000$ psi, $G = 100.0$ BSCF, $C_f = 4.0 \times 10^{-6}$ psi^{-1} , and various Ra/Rg .

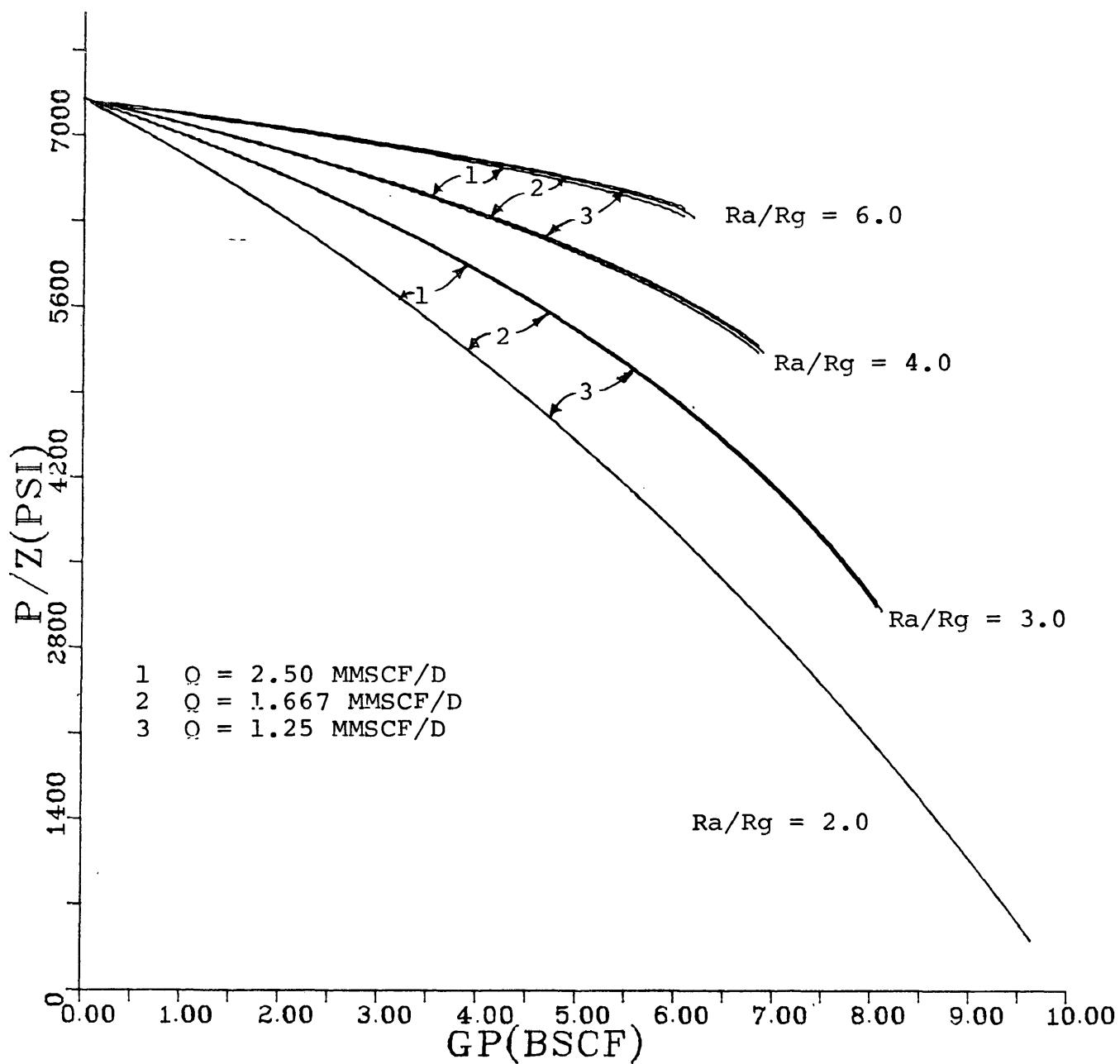


Figure 11. Effect of Field Production Rate on P/Z Performance, for $P_i = 10,000$ psi, $G = 10.0$ BSCF, $C_f = 4.0 \times 10^{-6}$ psi⁻¹, and various Ra/Rg.

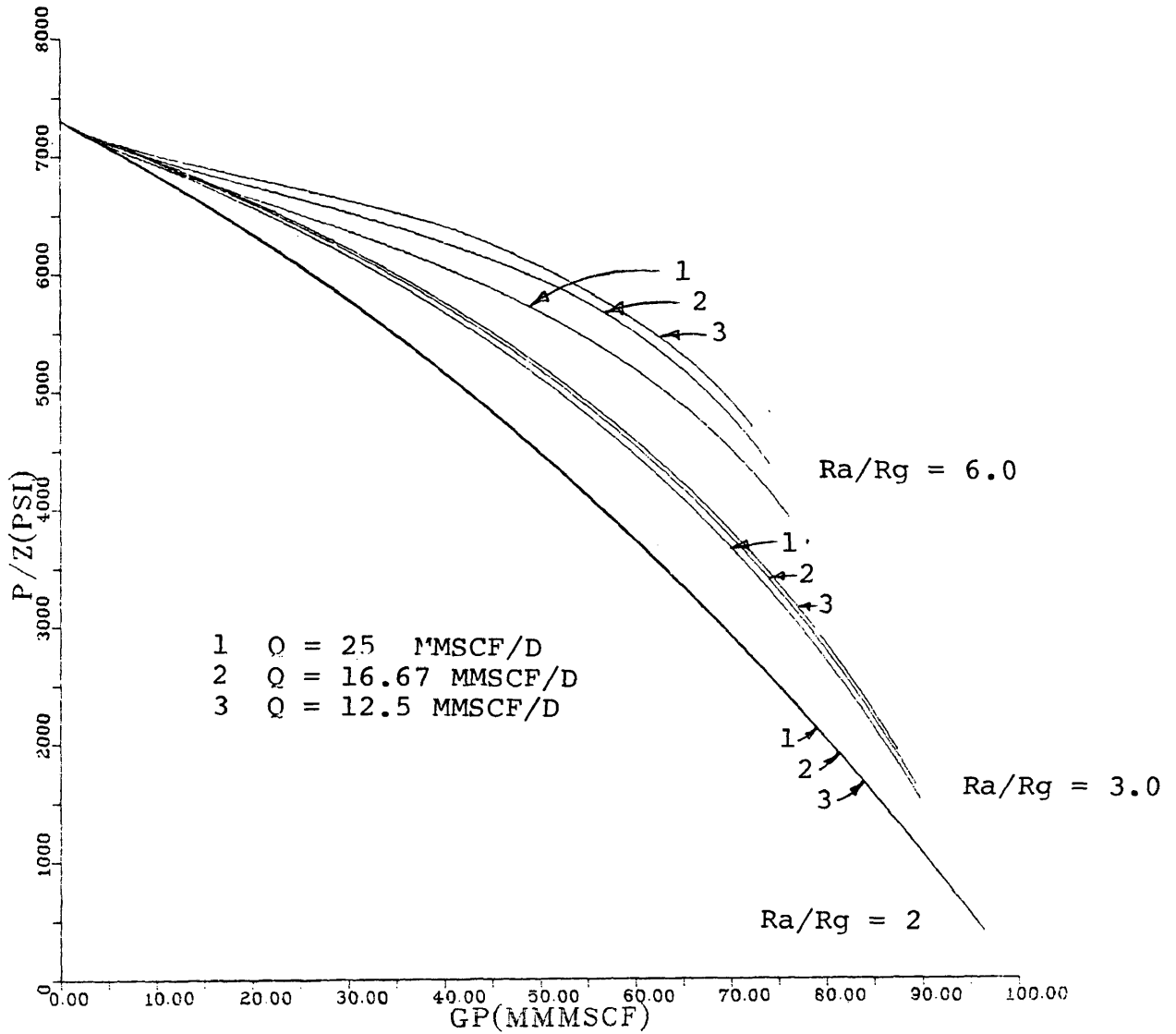


Figure 12. P/Z Performance, for $P_i = 10,000$ psi, various Ra/Rg , various field production rate, $G = 100.0$ BSCF, and $C_f = 4.0 \times 10^{-6}$ psi⁻¹.

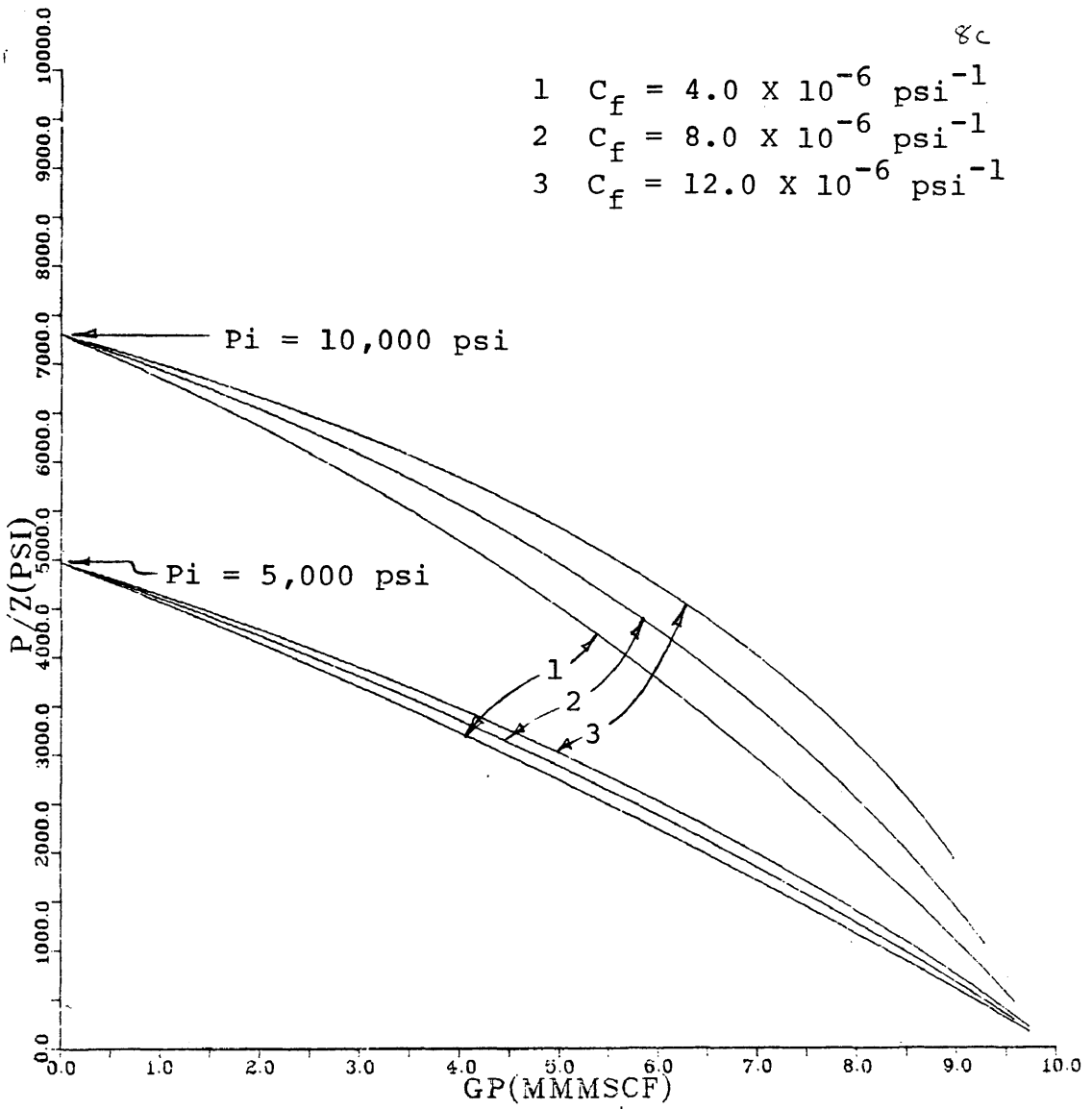


Figure 13. Effect of Formation Compressibility on the P/Z Performance for $P_i = 5,000 \text{ psi}$, $P_i = 10,000 \text{ psi}$, $G = 10.0 \text{ BSCF}$, $Q = 2.50 \text{ MMSCF/D}$, and $R_a/R_g = 2.0$.

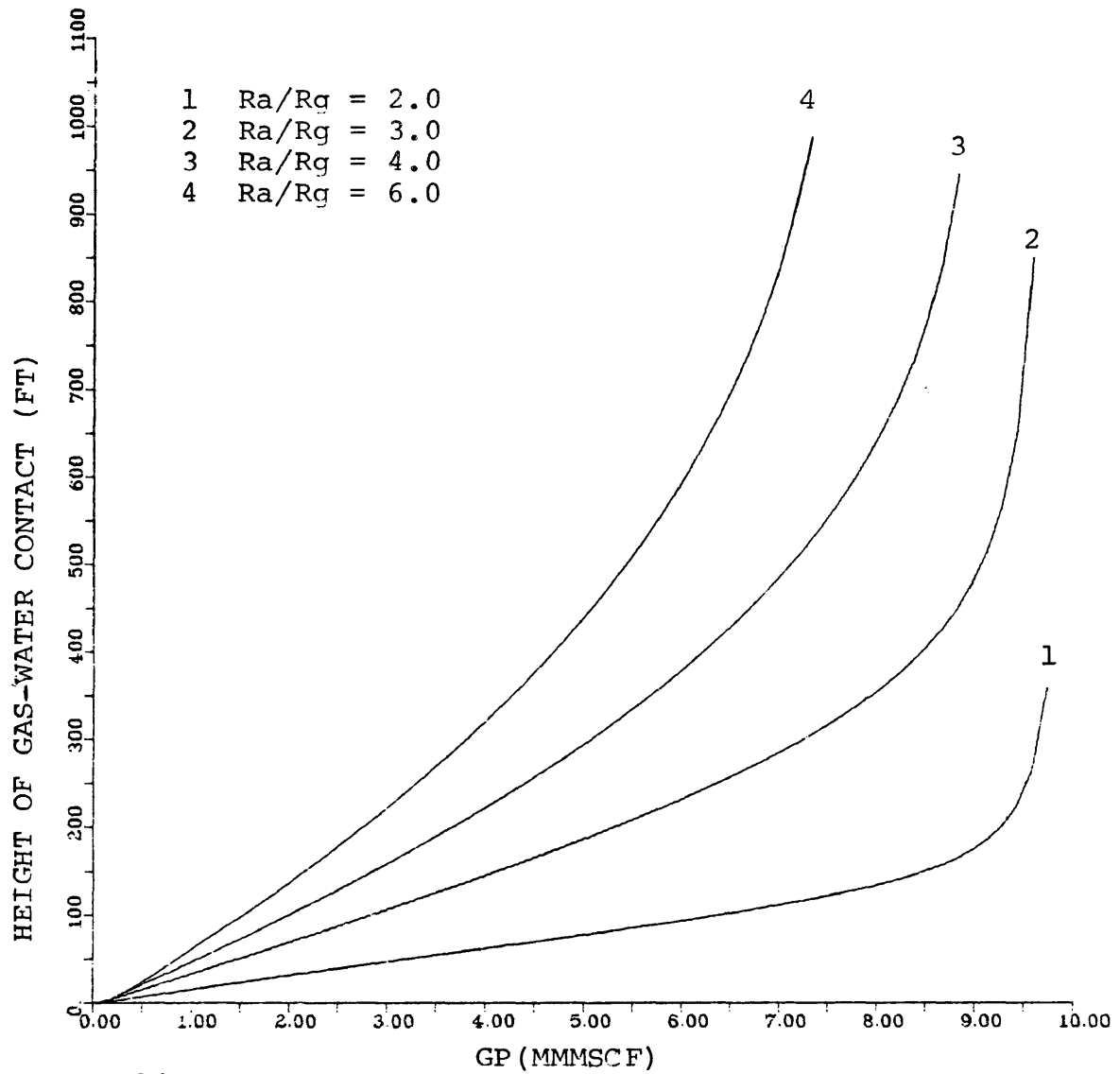


Figure 14. Gas-Water Contact Performance for $P_i = 5000$ psi, $G = 10.0$ BSCF, $Q = 2.5$ MMSCF/D, and $C_f = 4.0 \times 10^{-6}$ psi $^{-1}$.

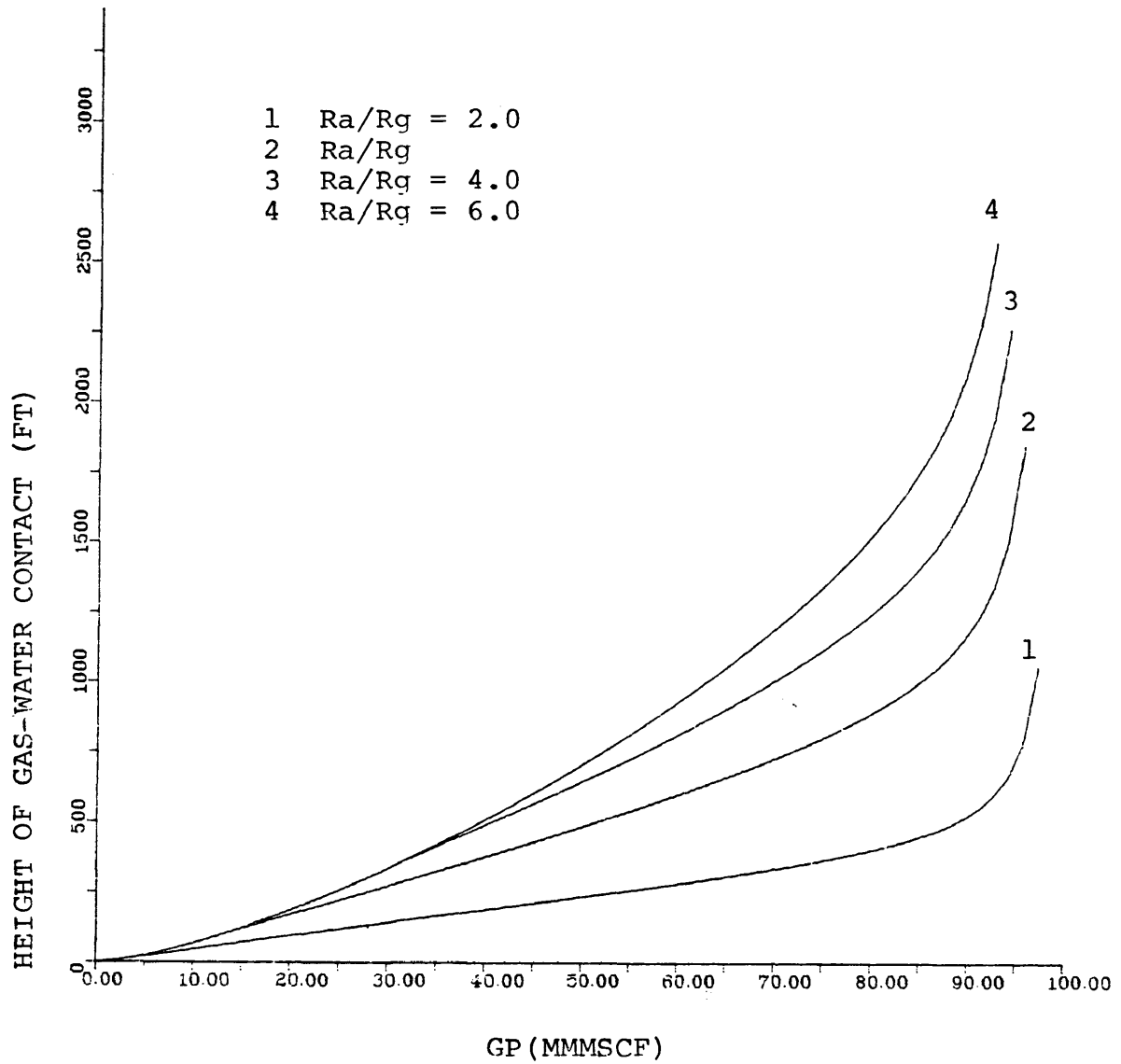


Figure 15. Gas-Water Contact Performance for $P_i = 5,000$ psi, $G = 100.0$ BSCF, $Q = 25.0$ MMSCF/D, $C_f = 4.0 \times 10^{-6}$ psi⁻¹, and various R_a/R_g .

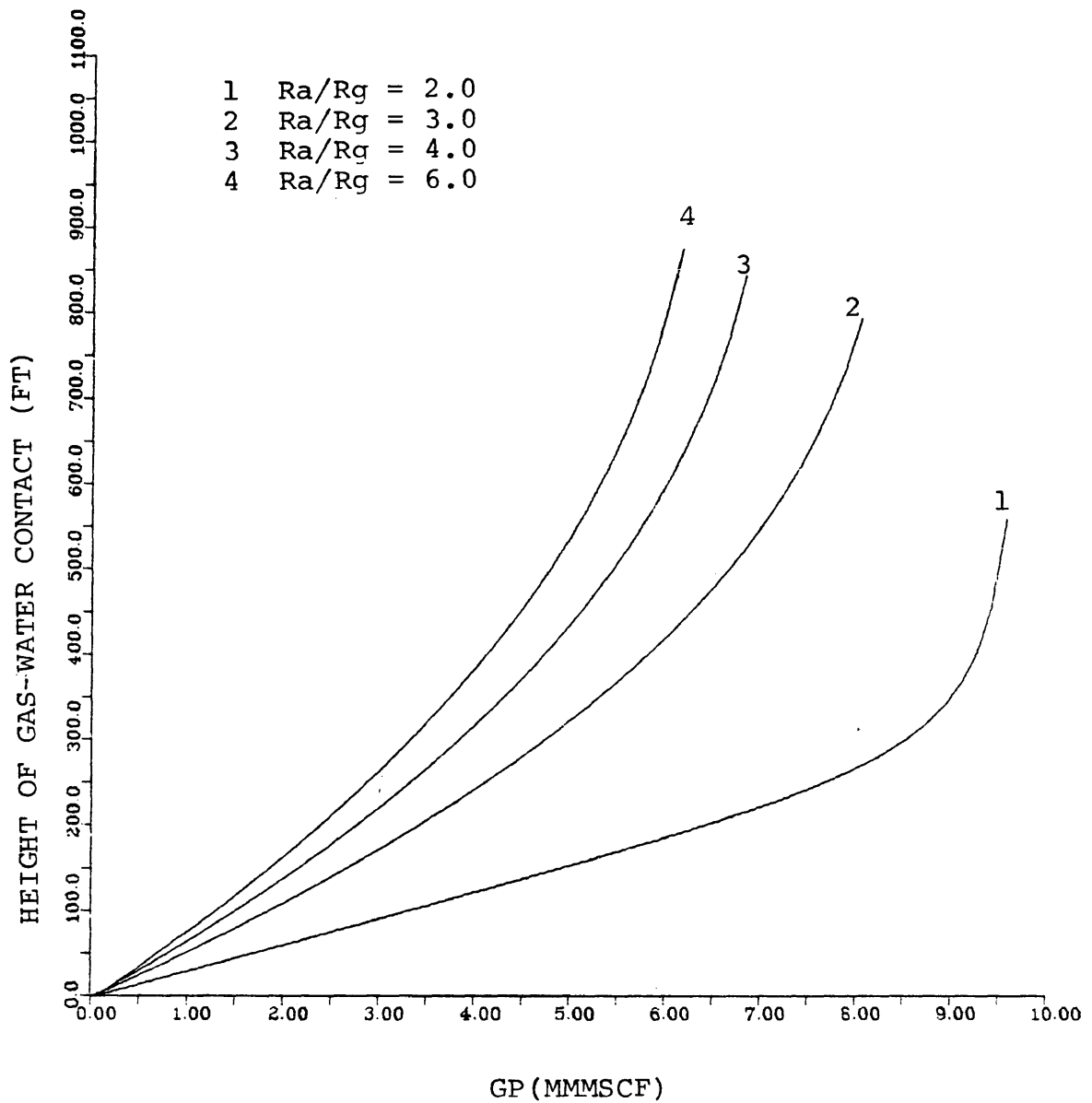


Figure 16. Gas-Water Contact Performance, for $P_i = 10,000$ psi, $G = 10.0$ BSCF, $Q = 2.50$ MMSCF/D, $C_f = 4.0 \times 10^{-6}$ psi $^{-1}$, and various Ra/Rg .

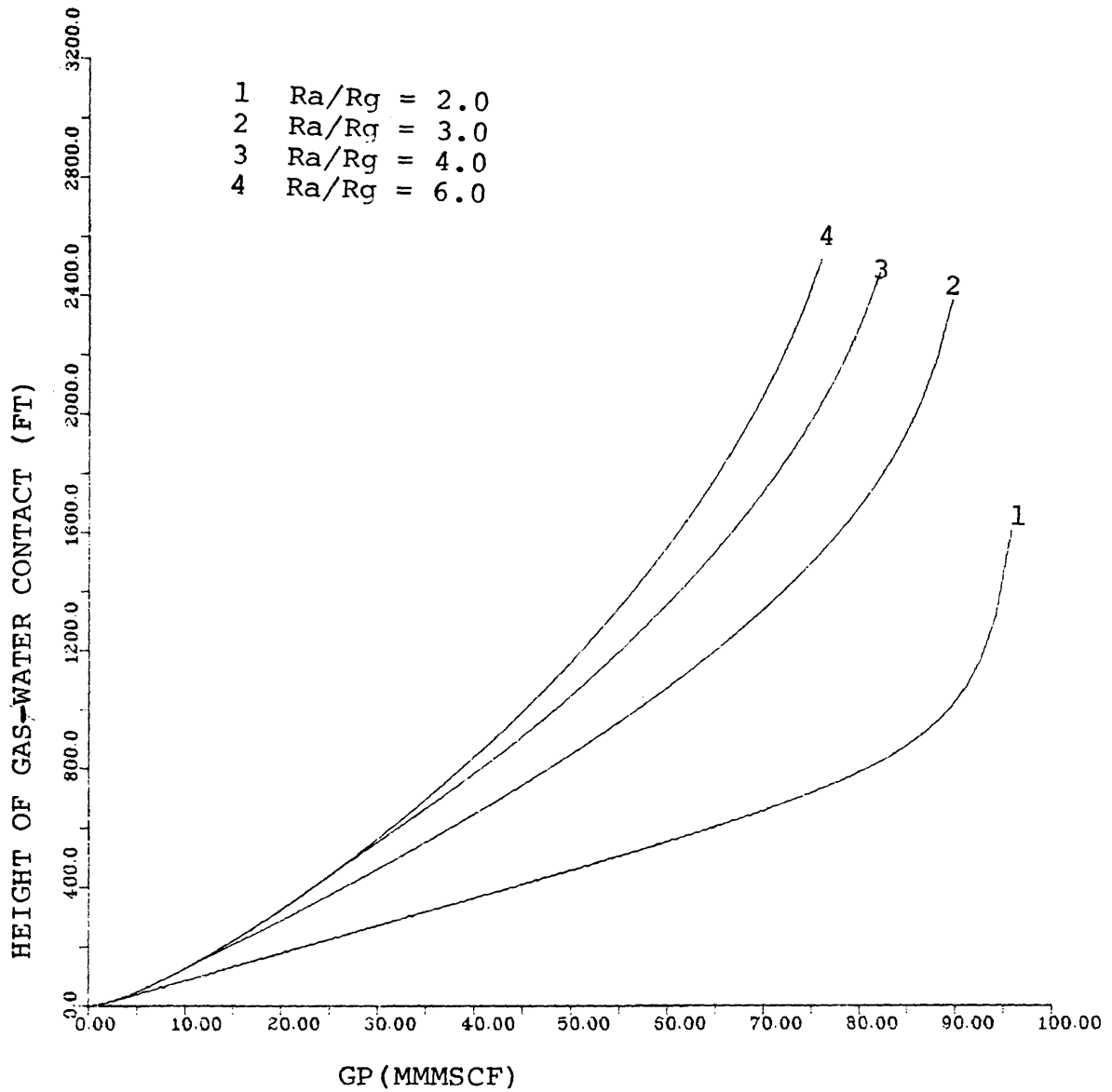


Figure 17. Gas-Water Contact Performance for $P_i = 10,000$ psi, $G = 100$ BSSF, $Q = 25.0$ MMSCF/D, $C_f = 4.0 \times 10^{-6}$ psi $^{-1}$, and various R_a/R_g .

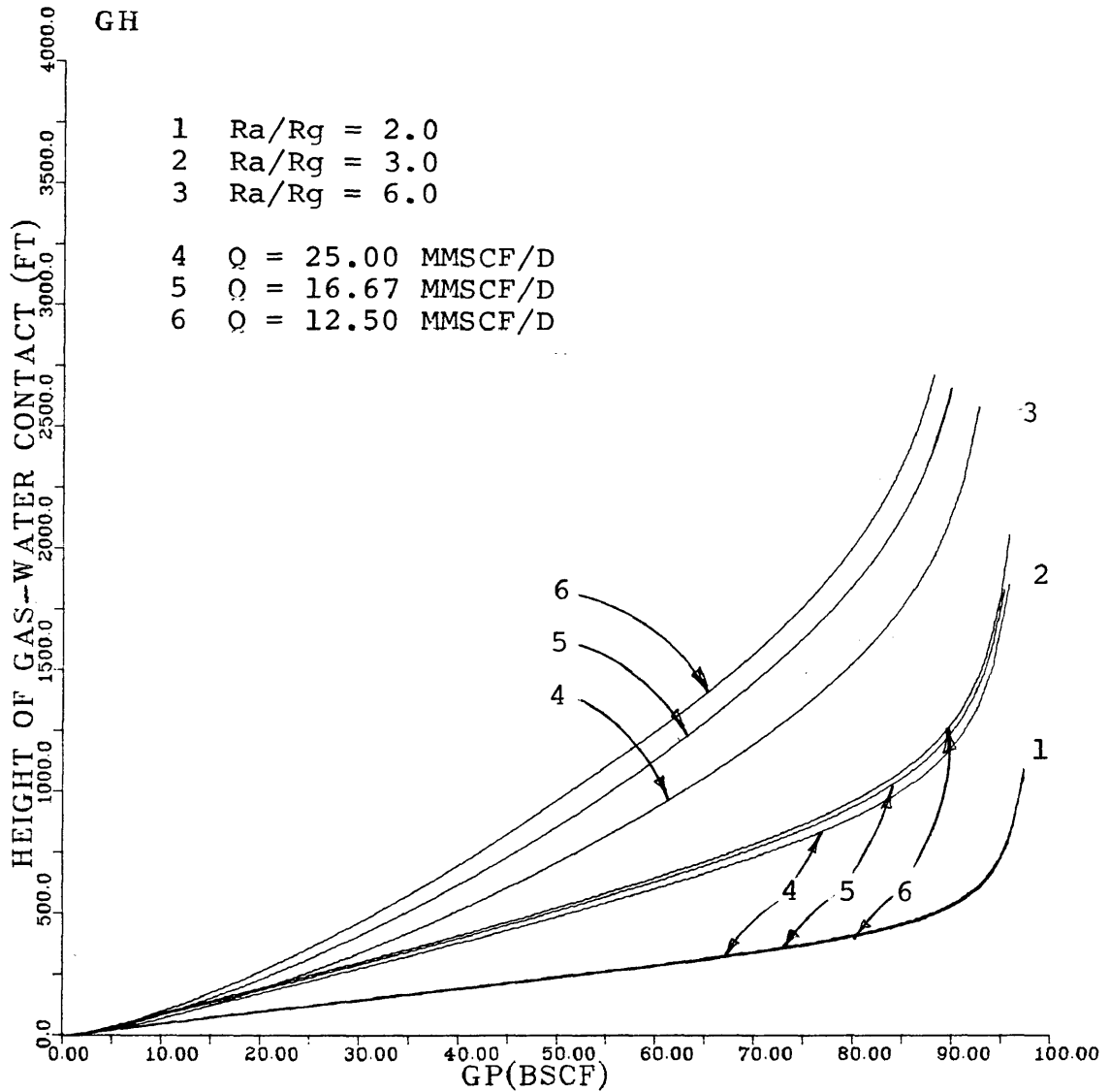


Figure 18. Effect Field Production Rate on the Gas-Water Contact Performance for $P_i = 5000$ psi, $G = 100.0$ BSCF, $C_f = 4.0 \times 10^{-6}$ psi⁻¹, and various R_a/R_g .

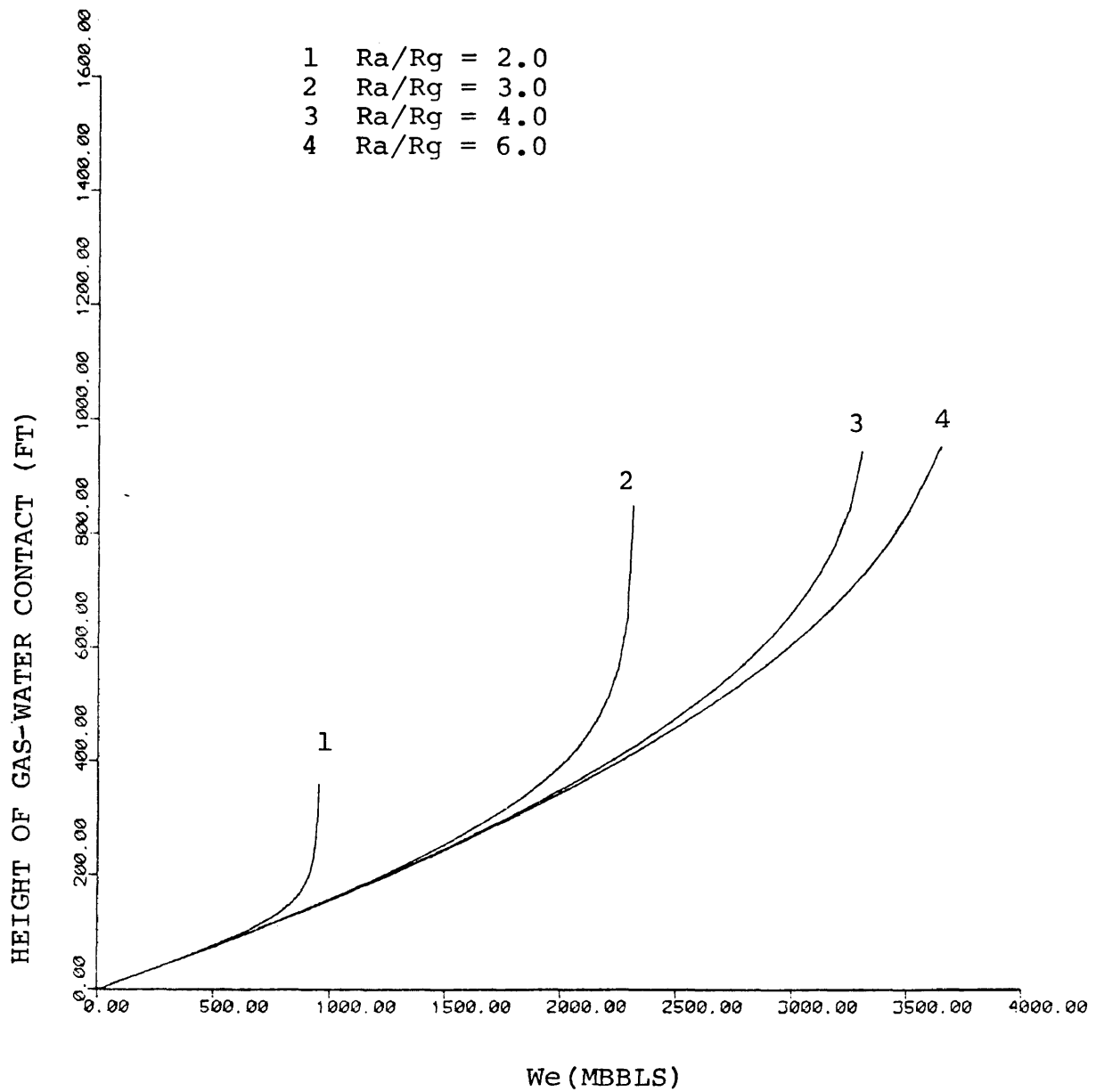


Figure 19. Effect of Ra/Rg on (We - Gas-Water contact)
 Performance for $P_i = 5,000$ psi, $G = 10.0$ BSCF,
 $Q = 2.5$ MMSCF/D, and $C_f = 4.0 \times 10^{-6}$ psi $^{-1}$.

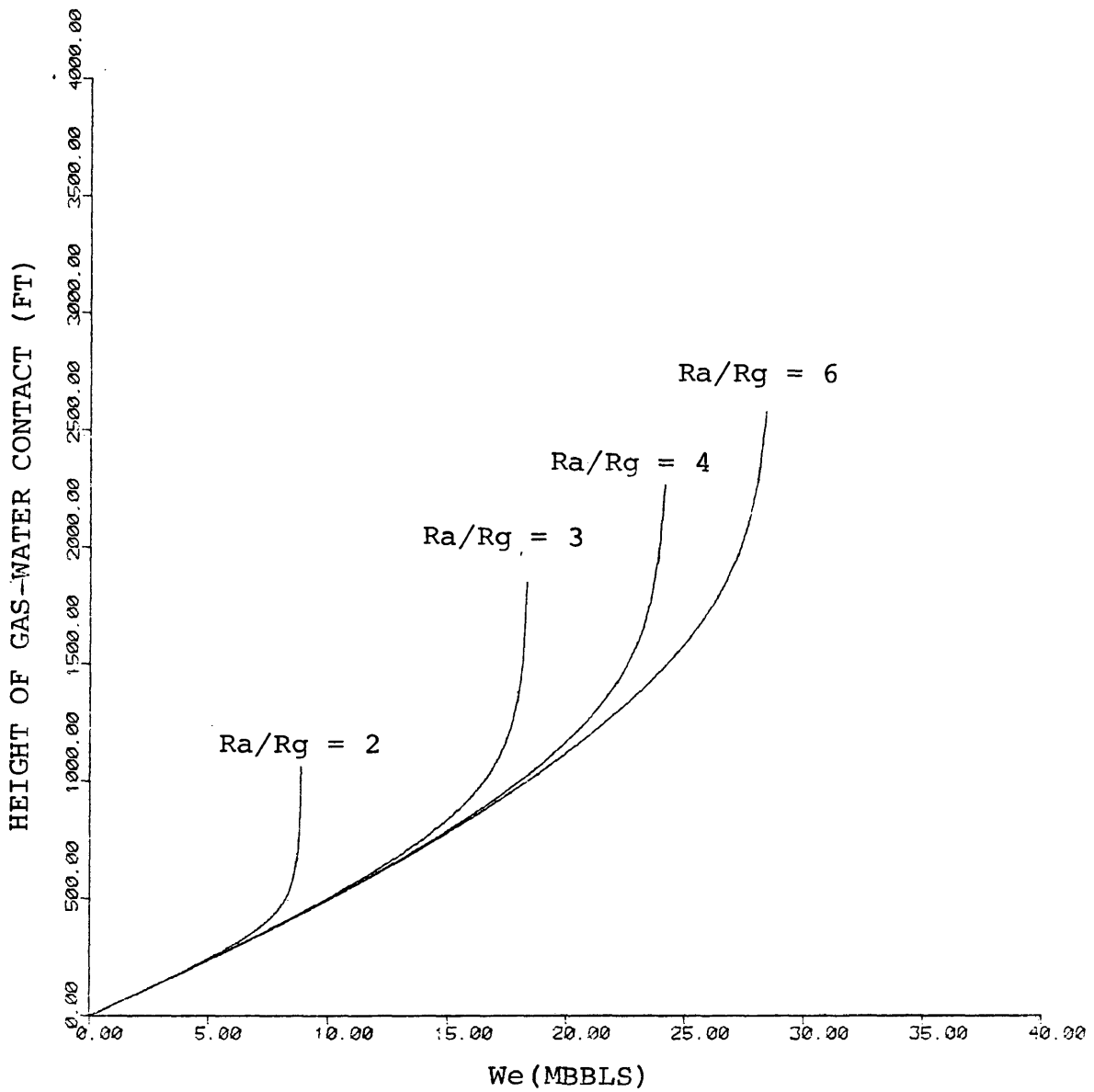


Figure 20. Effect of R_a/R_g on (We - G-W Contact)
Performance for $P_i = 5,000$ psi, $G = 100.0$ BSCF,
 $Q = 25.0$ MMSCF/D, and $C_f = 4.0 \times 10^{-6}$ psi⁻¹.

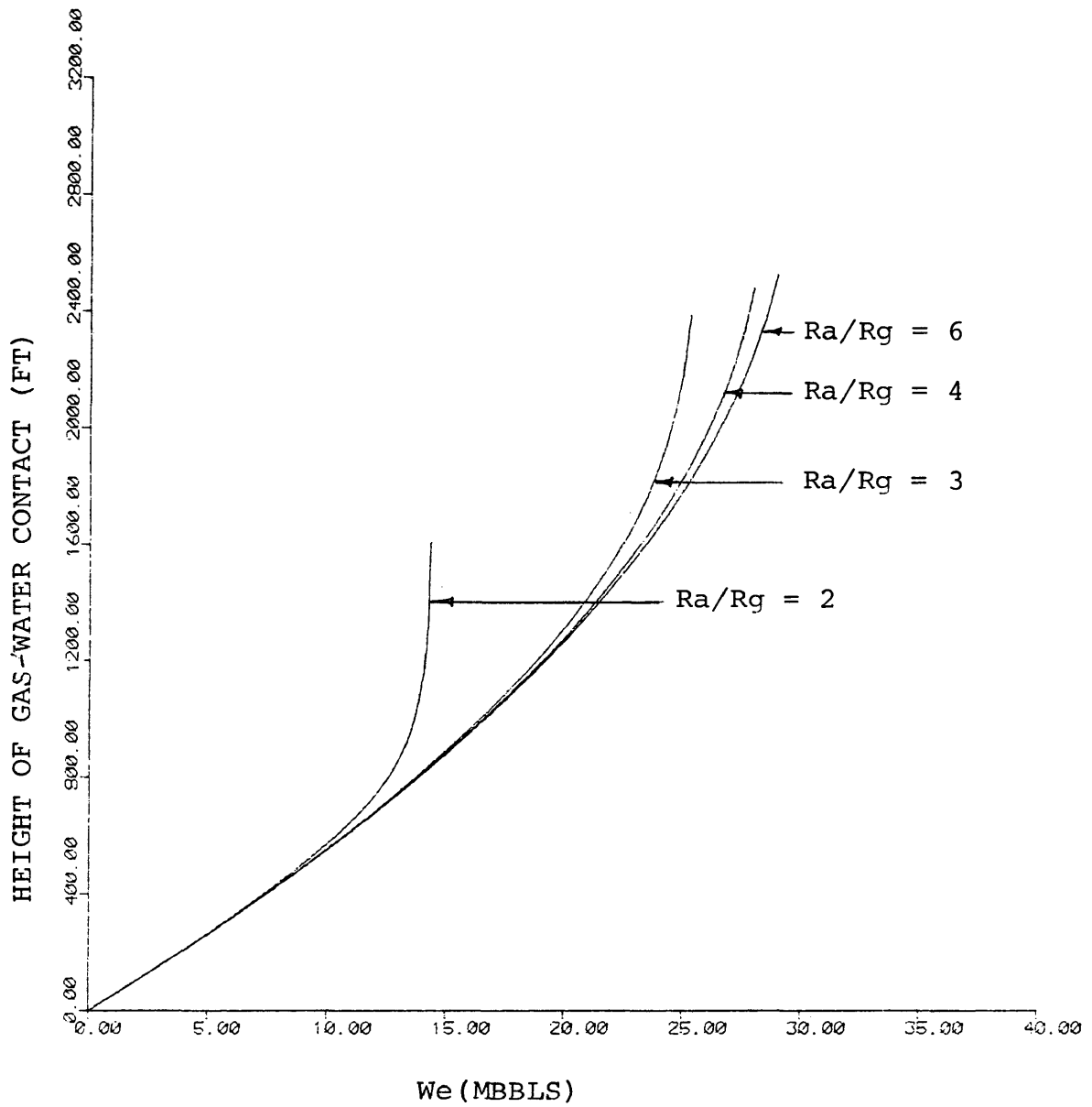


Figure 21. Effect of R_a/R_g on (W_e - Gas-water contact)
 Performance for $P_i = 10,000$ psi, $G = 100.0$ BSCF,
 $Q = 25.0$ MMSCF/D, and $C_f = 4.0 \times 10^{-6}$ psi $^{-1}$.

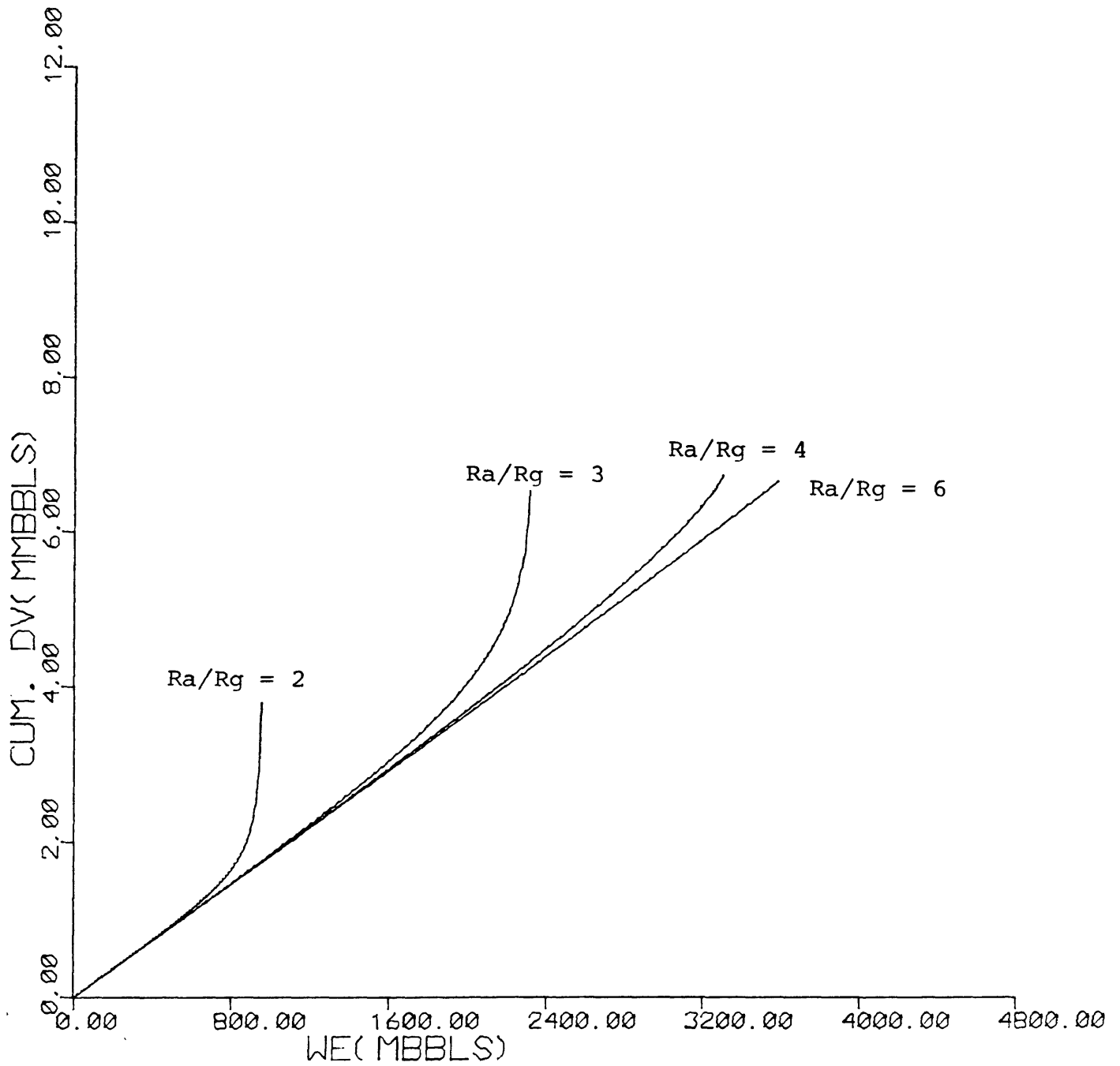


Figure 22. Effect of Ra/Rg on (We - cum. pore volume invaded) Performance, for $P_i = 5000$ psi, $G = 10.0$ BSCF, $Q = 2.5$ MMSCF/D, and $C_f = 4.0 \times 10^{-6}$ psi⁻¹.

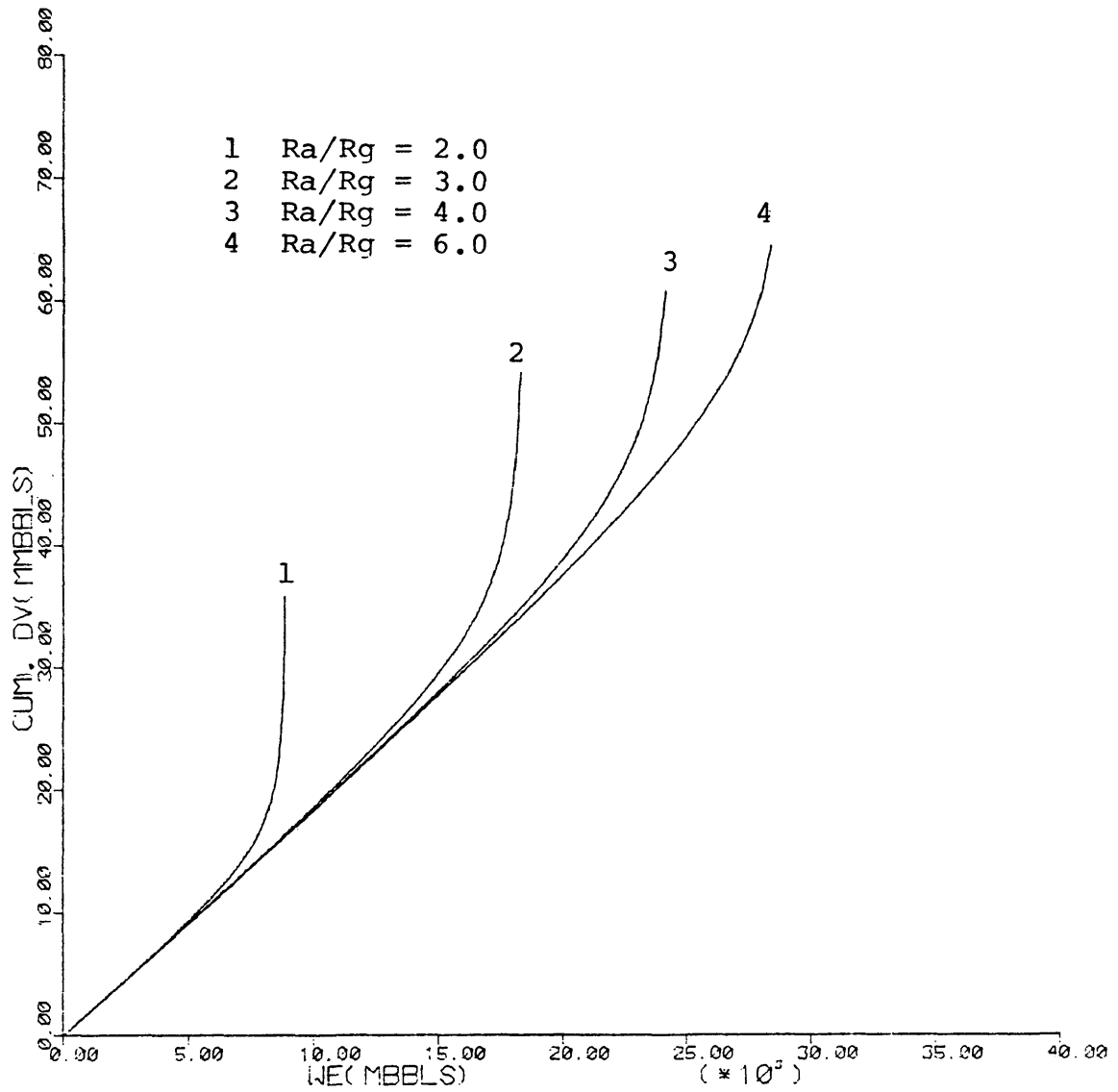


Figure 23. Effect of R_a/R_g on (We - Cum. Pore Volume Invaded) Performance, For $P_i = 5,000$ psi, $G = 100.0$ BSCF, $Q = 25$ MMSCF/D, and $C_f = 4.0 \times 10^{-6}$ psi $^{-1}$.

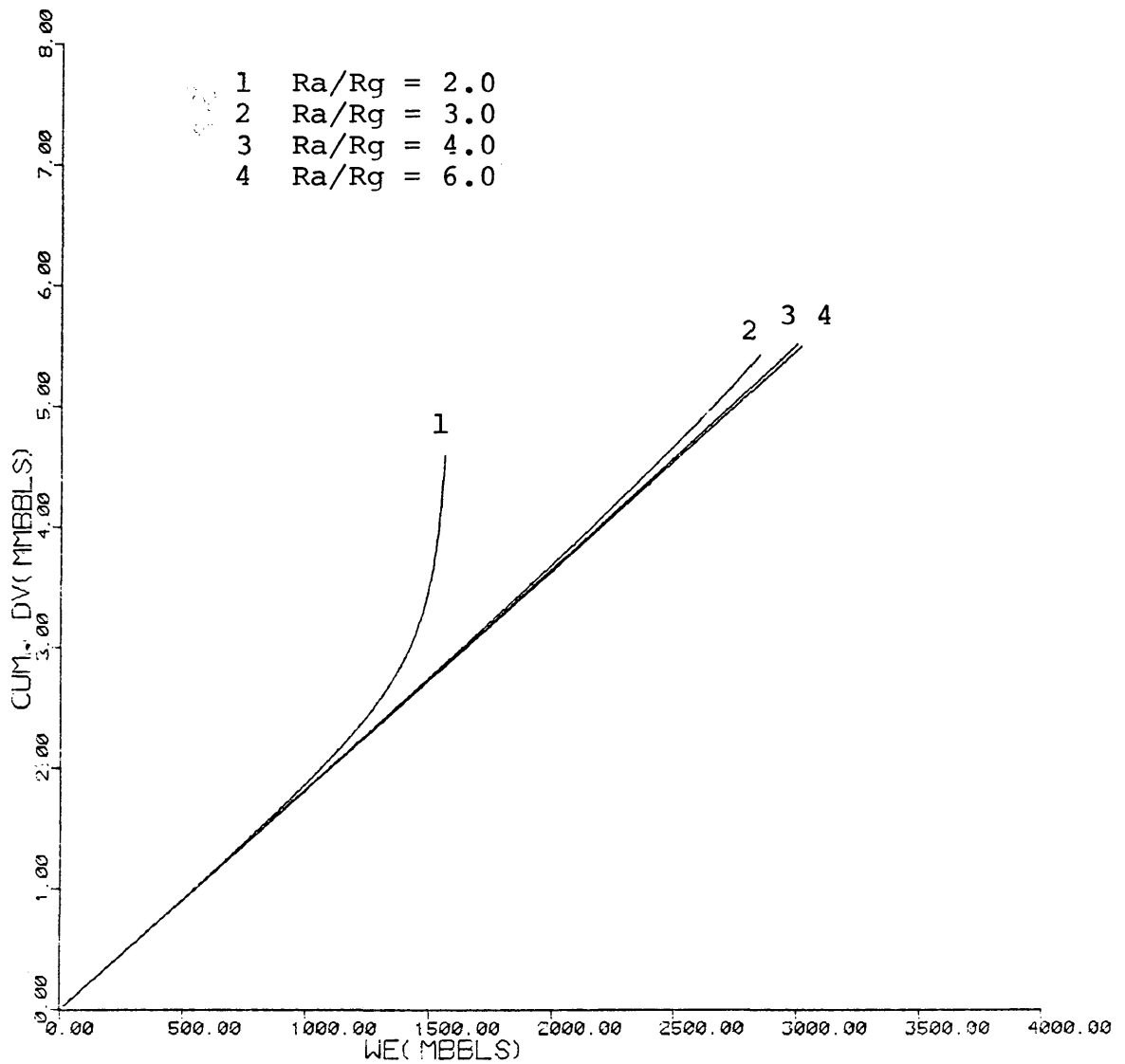


Figure 24. Effect of R_a/R_g on (We - Cum. Pore Volume Invaded) Performance for $P_i = 10,000$ psi, $G = 10.0$ BSCF, $Q = 2.5$ MMSCF/D, and $C_f = 4.0 \times 10^{-6}$ psi $^{-1}$.

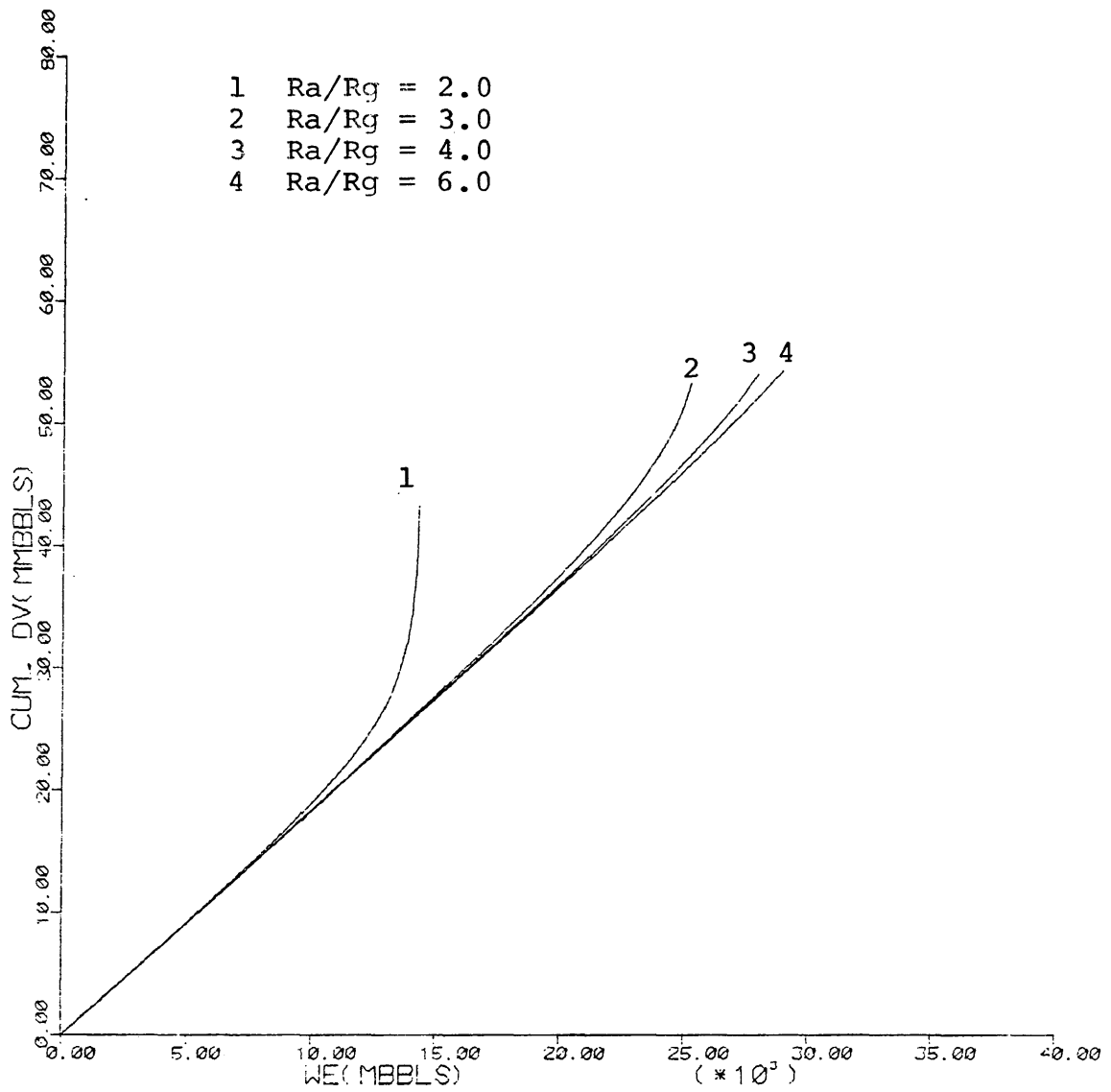


Figure 25. Effect of R_a/R_g on (We - Cum. Pore Volume Invaded) Performance for $P_i = 10,000$ psi, $G = 100.0$ BSCF, $Q = 25$ MMSCF/D, and $C_f = 4.0 \times 10^{-6}$ psi $^{-1}$.

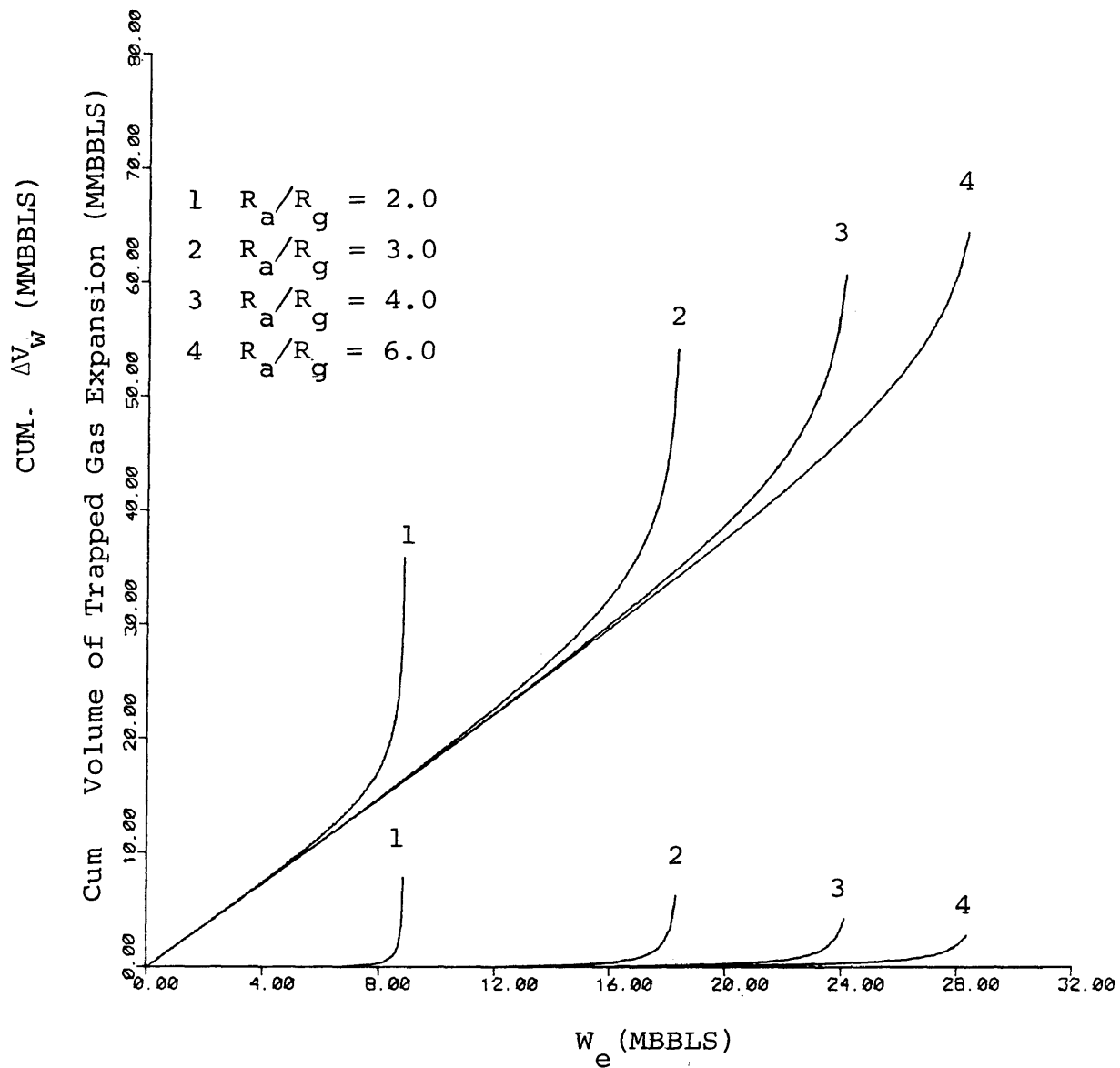


Figure 26. Effect of the expansion of the trapped gas in the water invaded zone on the cumulative volume invaded. For $P_i = 4,000$ psi, $G = 100$ BSCF, $Q = 25$ MMSCF/D, $C_f = 4.0 \times 10^{-6}$ psi $^{-1}$, and various R_a/R_g . (The upper set represents the cumulative pore volume invaded and the lower set represents the associated gas expansion of the trapped gas in the water invaded zone.)

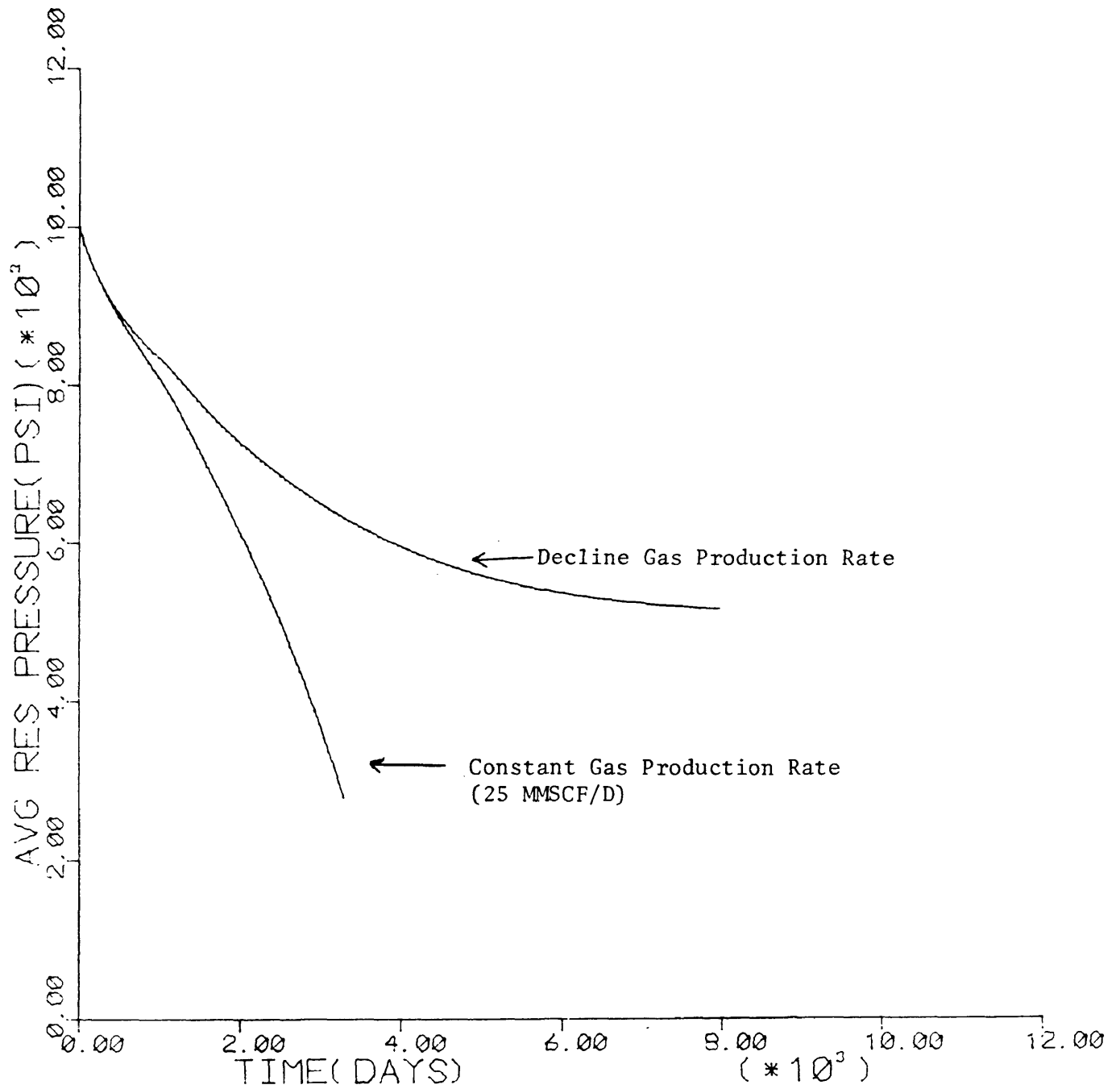


Figure 27. Effect of Constant and Decline Gas Production Rate on the Performance of Average Gas Reservoir Pressure for $P_i = 10,000$ psi, $G = 100$ BSCF, $C_f = 4.0 \times 10^{-6}$ psi⁻¹, and $R_a/R_g = 4.0$.

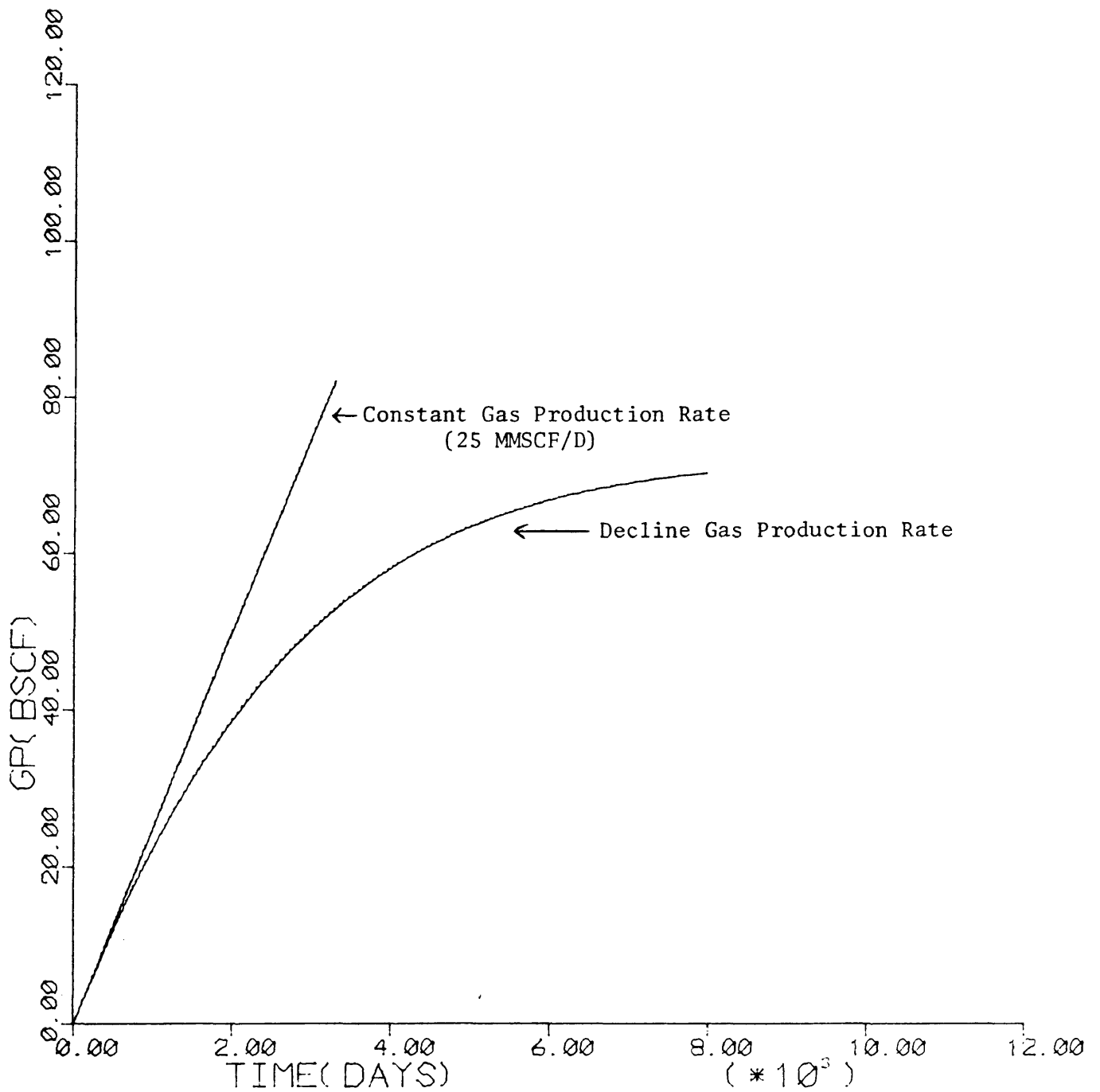


Figure 28. Effect of Constant and Decline Gas Production Rate on the Cumulative Gas Recovery for $P_i = 10,000$ psi, $G = 100$ BSCF, $C_f = 4.0 \times 10^{-6}$ psi $^{-1}$, and $R_a/R_g = 4.0$.

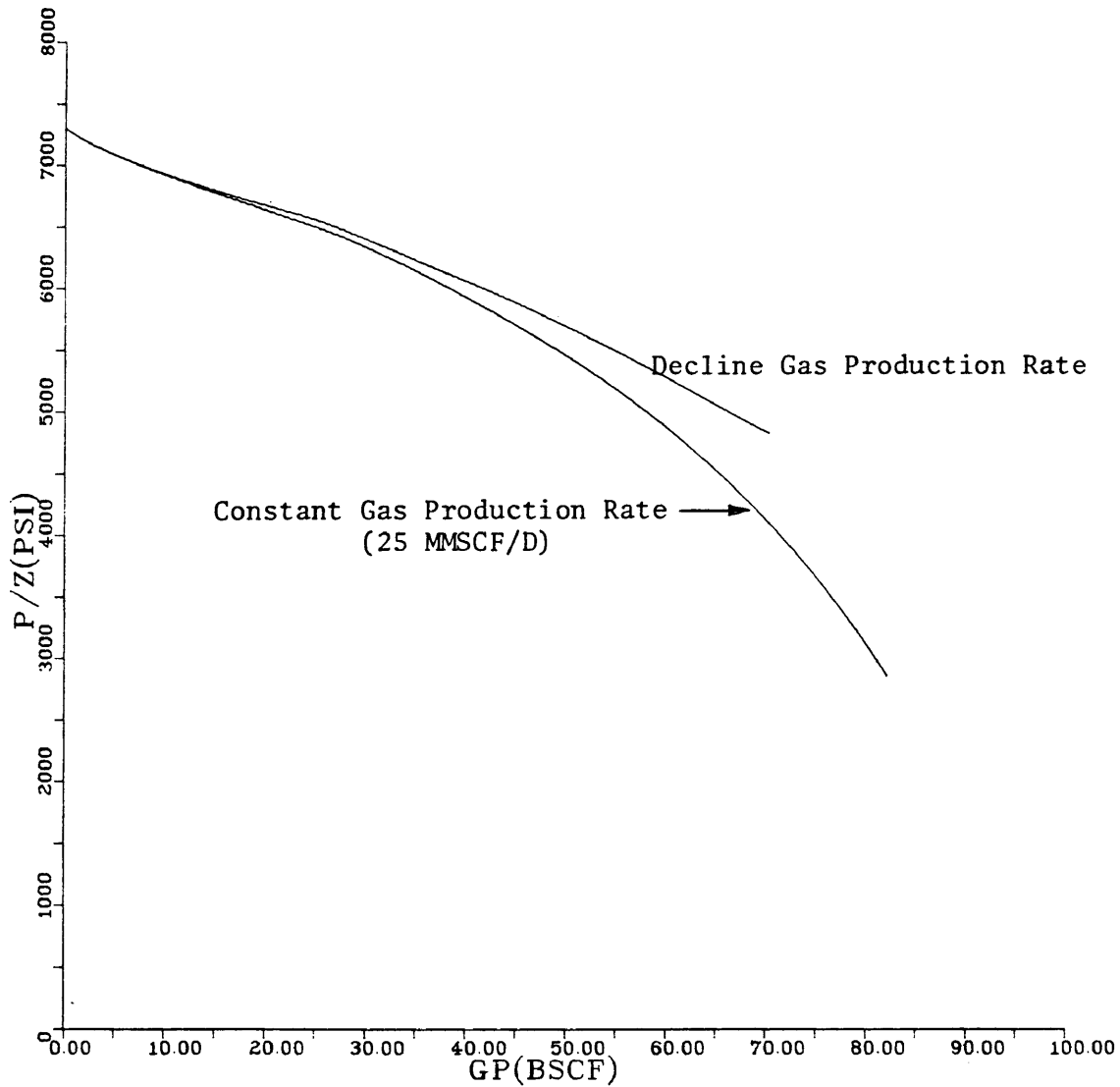


Figure 29. Effect of Constant and Decline Gas Production Rate on the P/Z Performance for $P_i = 10,000$ psi, $G = 100$ BSCF, $C_f = 4.0 \times 10^{-6}$ psi $^{-1}$ and $R_a/R_g = 4.0$.

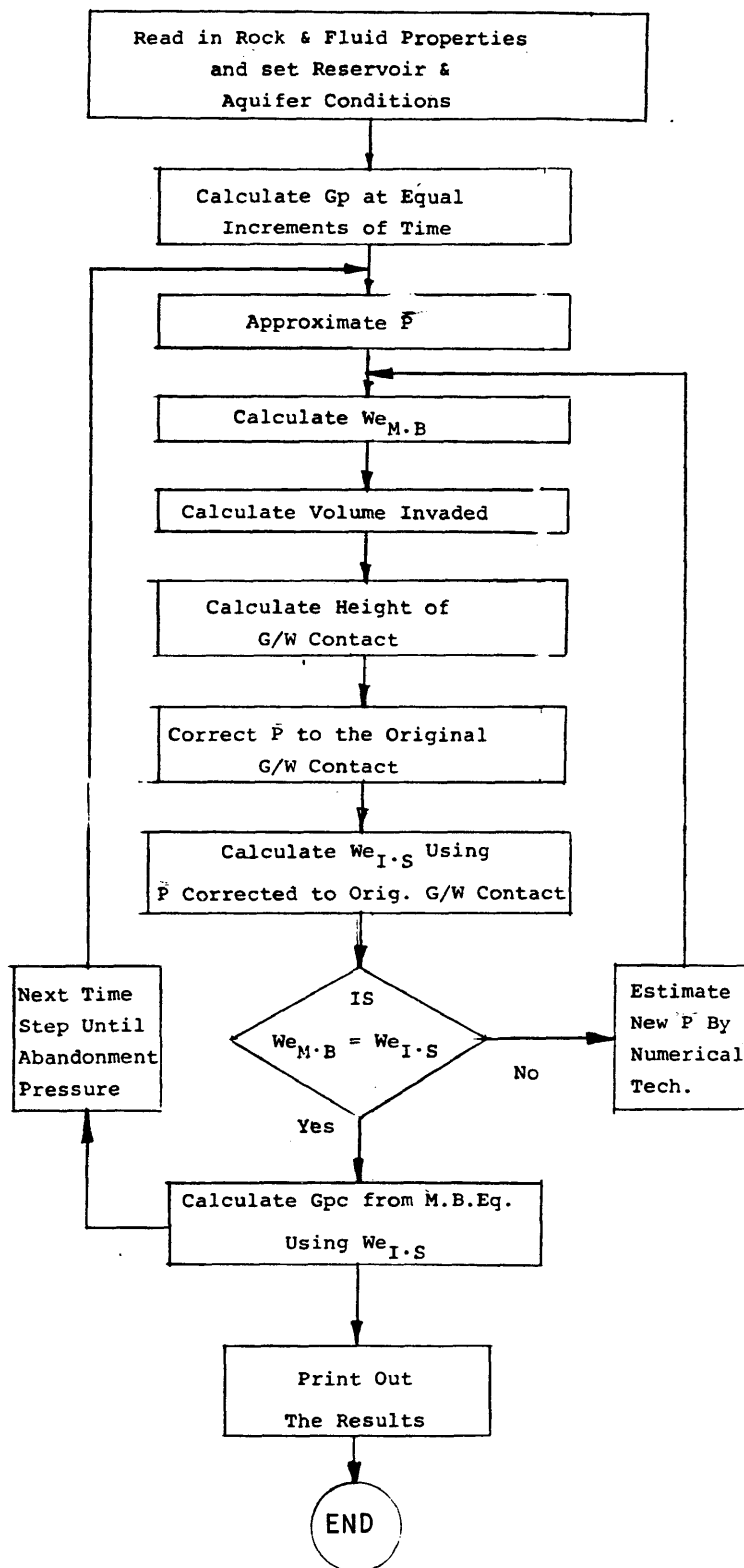


Figure 30. Simplified Flow Diagram of Calculation Procedure

ACKNOWLEDGEMENT

The author wishes to express his greatfull appreciation to Dr. D.M. Bass, Head of the Department of Petroleum Engineering, Colorado School of Mines, and thesis advisor for suggesting the topic and for his valuable suggestions and guidance throughout this work. The author wishes also to express his sincere thanks to Dr. D.W. Hilchie and Prof. D.I. Dickinson for serving on his committee.

REFERENCES

1. Bass, D.M., 1978, PE 512 class notes.
2. Bass, D.M., 1978, PE 607 class notes.
3. Craft, B.C., and Hawkins, M.F.: Applied Petroleum Reservoir Engineering, Prentice-Hall, Inc., Englewood Cliffs, N.J. 1959.
4. Van-Everdingen, A.F., Timmerman, E.H., and McMahon, J.J.: Application of the Material Balance Equation To A Partial Water Drive Reservoir, Trans., AIME (1953), 187,51.
5. Bruns, J.R., Fetkovich, M.J., Meitzen, V.C.: The Effect of Water Influx on P/Z - Cumulative Gas Production Curves, Jour. Pet. Tech. (March, 1965) 287.
6. Shagroni, M.A.: Effect of Formation Compressibility and Edge Water on Gas Field Performance, Master of Engineering, Colorado School of Mines, 1977.
7. Agarwal, R.G., Al-Hussainy, R., Ramey, H.J.: The Importance of Water Influx in Gas Reservoir, Jour. Pet. Tech. (November 1965) 1336.
8. Dumoré, J.M.: Material Balance for a Bottom-Water Drive Gas Reservoir, Soc. Pet. Eng. J., (Dec. 1973).
9. Rossen, R.H.: A Regression Approach to Estimate Gas In Place For Gas Fields, Jour. Pet. Tech. (October 1975) 1283-1289.
10. Van-Everdingen, A.F., and Hurst, W.: The Application of the Laplace Transformation to Flow Problems in Reservoirs, Trans., AIME (1949) 186,305.
11. Colorado School of Mines programs library: 1) Water influx subroutine, 2) Z-factor subroutine, 3) Pseudo-reduced properties subroutine.
12. Geffen, T.M., Parrish, D.R., Haynes G.W., and Morse, R.A.: Efficiency of Gas Displacement From Porous Media By Liquid Flooding, Trans., AIME (1952) 195, 29.
13. Pepperdine, L.: The Recognition and Evaluation of Water Drive Gas Reservoirs, Petroleum Society of CIM, Paper No. 78-29.38 (1978).
14. Givens, J.W.: A Practical Two-Dimensional Model for Simulating Dry Gas Reservoirs With Bottom Water Drive, J. Pet. Tech. (November 1968) 1229-1233.